

# Water Resources Research

## RESEARCH ARTICLE

10.1029/2019WR025967

### Key Points:

- Upslope groundwater data do not show diel fluctuations, suggesting that upslope vegetation does not contribute to streamflow fluctuations
- Transpiration-driven diel fluctuations in near-stream groundwater vary spatially due to changes in estimated bedrock permeability and depth to groundwater
- Amplitudes of diel fluctuations in near-stream groundwater increase through the summer, as trees increase use as soil water decreases

### Supporting Information:

- Figure S1

### Correspondence to:

R. Harmon,  
ryanharmon@mines.edu

### Citation:

Harmon, R., Barnard, H. R., & Singha, K. (2020). Water table depth and bedrock permeability control magnitude and timing of transpiration-induced diel fluctuations in groundwater. *Water Resources Research*, 56, e2019WR025967. <https://doi.org/10.1029/2019WR025967>

Received 12 JUL 2019

Accepted 25 MAR 2020

Accepted article online 26 MAR 2020

## Water Table Depth and Bedrock Permeability Control Magnitude and Timing of Transpiration-Induced Diel Fluctuations in Groundwater

Ryan Harmon<sup>1</sup> , Holly R. Barnard<sup>2</sup> , and Kamini Singha<sup>1</sup> 

<sup>1</sup>Hydrologic Science and Engineering, Colorado School of Mines, Golden, CO, USA, <sup>2</sup>Institute of Arctic and Alpine Research, Department of Geography, University of Colorado, Boulder, CO, USA

**Abstract** The subsurface processes that mediate the connection between evapotranspiration and groundwater within forested hillslopes are poorly defined. Here, we investigate the origin of diel signals in unsaturated soil water, groundwater, and stream stage on three forested hillslopes in the H.J. Andrews Experimental Forest in western Oregon, USA, during the summer of 2017, and assess how the diurnal signal in evapotranspiration (ET) is transferred through the hillslope and into these stores. There was no evidence of diel fluctuations in upslope groundwater wells, suggesting that tree water uptake in upslope areas does not directly contribute to the diel signal observed in near-stream groundwater and streamflow. The water table in upslope areas resided within largely consolidated bedrock, which was overlain by highly fractured unsaturated bedrock. These subsurface characteristics inhibited formation of diel signals in groundwater and impeded the transfer of diel signals in soil moisture to groundwater because (1) the bedrock where the water table resides limited root penetration and (2) the low unsaturated hydraulic conductivity of the highly fractured rock weakened the hydraulic connection between groundwater and soil/rock moisture.

Transpiration-driven diel fluctuations in groundwater were limited to near-stream areas but were not ubiquitous in space and time. The depth to the groundwater table and the geologic structure at that depth likely dictated rooting depth and thus controlled where and when the transpiration-driven diel fluctuations were apparent in riparian groundwater. This study outlines the role of hillslope hydrogeology and its influence on the translation of evapotranspiration and soil moisture fluctuations to groundwater and stream fluctuations.

**Plain Language Summary** In many groundwater-fed streams, tree water uptake can create daily fluctuations in streamflow. The lowest value in these fluctuations, occurring during the afternoon or early evening, typically correspond to the maximum tree water uptake, while the peaks correspond to minimum tree water uptake during the night. The presence of these fluctuations in streamflow suggests that trees and streams are closely connected; however, because of limited access to the subsurface it is difficult to determine how these fluctuations propagate through the hillslope and into the stream. We found that trees in upslope areas rely on soil water that is hydraulically disconnected from groundwater, and thus fluctuations from transpiration are not transferred to groundwater and the stream from upslope. The creation of daily fluctuations in groundwater was limited to near-stream areas. By identifying the physical processes that control the expression of these transpiration signals, we can improve our ability to determine the water reservoirs that trees rely on.

## 1. Introduction

The influences of geology and topography on the movement of water in the subsurface have been studied extensively (e.g., Freeze & Witherspoon, 1967; Gleeson & Manning, 2008; Rempe & Dietrich, 2014; Tóth, 1963; Winter, 2001), but how tree water uptake affects hydrologic flowpaths and subsurface water storage remains an open question (Brooks et al., 2015; Brantley et al., 2017). At the catchment scale, near-sinusoidal fluctuations in stream discharge—with a minimum occurring in the late afternoon and a maximum occurring in the early morning—have been attributed to evapotranspiration (ET) (e.g., Czikowsky & Fitzjarrald, 2004; Lundquist & Cayan, 2002; White 1932) (Figure 1a). Fluctuations in barometric pressure (Turk, 1975) and diel changes in water viscosity caused by changes in water temperature (Constantz & Zellweger, 1995; Constantz, 1998; Czikowsky & Fitzjarrald, 2004) have also been proposed

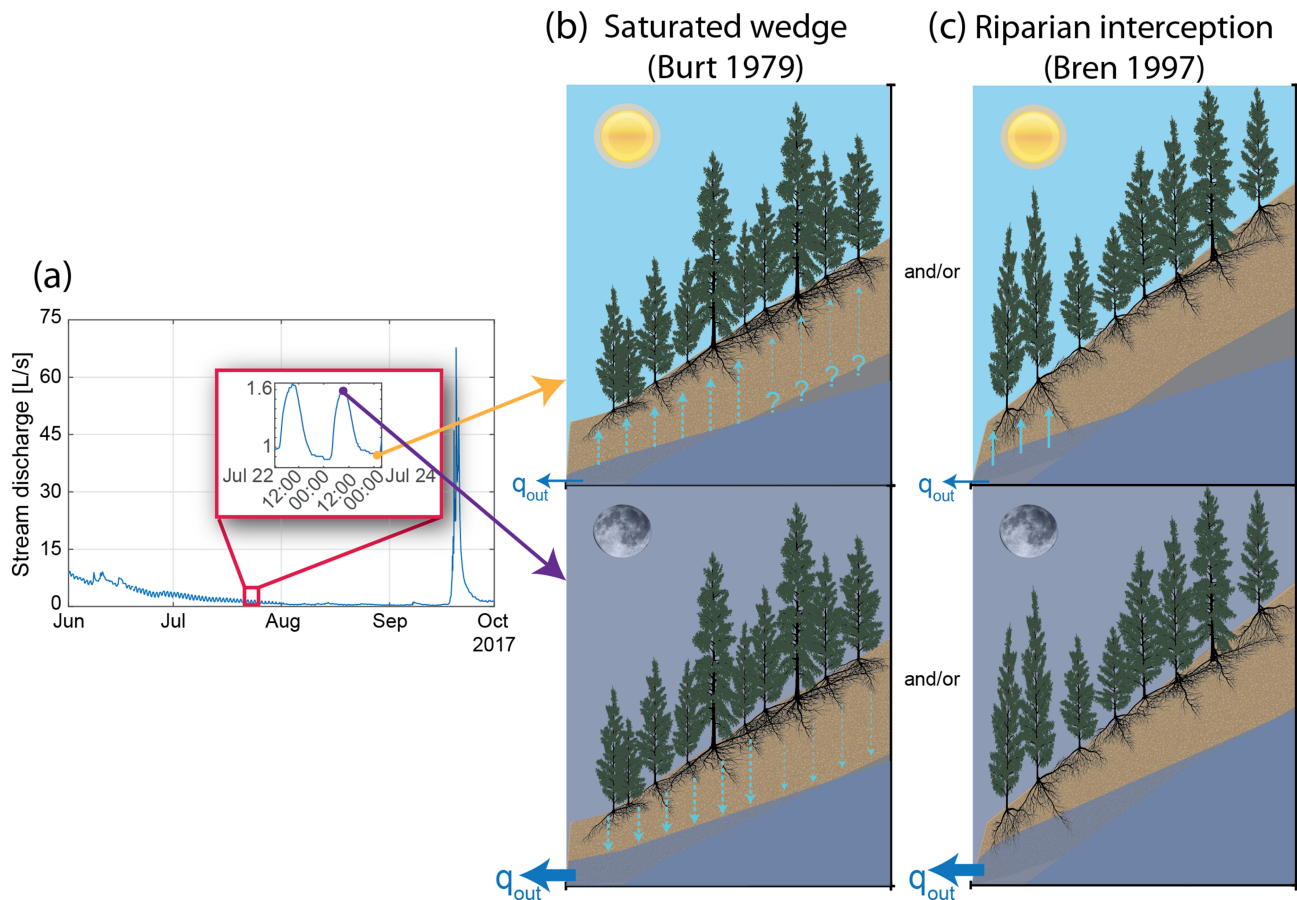


**Figure 1.** (a) Stream discharge ( $L s^{-1}$ ) measured at outlet of WS10 and an inset of diel fluctuations in stream discharge. Schematic of two basic conceptual models: (b) the saturated wedge hypothesis—diel fluctuations in ET, perhaps over the entire hillslope, drive diel changes in soil matric potential gradients, which lead to an upward daytime and downward nighttime migration of water through soil pore spaces, and (c) the riparian interception hypothesis—diel fluctuations result from riparian vegetation water use, which is directly intercepted from groundwater that is flowing toward the stream.

as contributing factors to diel fluctuations in stream discharge (Graham et al., 2013); however, these are often minor effects and can be accounted for, if needed, by monitoring barometric pressure and/or removing temperature effects (Moore et al., 2016). Transpiration-driven diel fluctuations in stream discharge have been observed in numerous catchments and can compromise over 10% of mean daily discharge in streams in the western United States (Lundquist & Cayan, 2002). However, due to the complex interactions among trees, hillslopes, aquifers, and streams, and the sparsity of subsurface data, no single conceptual model has accounted for the combined effects of multiple controlling variables on the expression of transpiration in subsurface water stores.

ET occurs over the entire catchment, yet many hypothesize that vegetation in the riparian zone is primarily responsible for the creation of diel fluctuations observed in near-stream groundwater and stream discharge (e.g., Loheide, 2008; Szilágyi et al., 2008; Széles et al., 2018; Yashi et al., 1990). Bren (1997) showed that when upslope vegetation was removed and a 30-m buffer of riparian vegetation was retained, diel fluctuations in stream discharge not only persisted but also increased in amplitude. These findings were used to develop the riparian interception hypothesis, which posits that upper hillslope vegetation does not contribute to the observed diel signals; rather, riparian vegetation intercepts water moving toward the stream from lateral subsurface flowpaths or from the groundwater table, leading to diel changes in discharge (Figure 1c). However, when Dunford and Fletcher (1947) removed near-stream vegetation, diel fluctuations in streamflow did not disappear as noted by Bren (1997); they instead observed a dampened diel signal in streamflow, suggesting that both riparian and upslope vegetation contribute to diel signals in stream discharge. Similarly, Burt (1979) found strong diel fluctuations in the stream discharge and in the lateral subsurface flow on a

hillslope with upslope vegetation that lacked near-stream vegetation. These findings led to the development of a second hypothesis used to explain the formation of diel fluctuations—the saturated wedge hypothesis—that suggests that the hillslope trees can contribute to the formation of the diel signal in groundwater flow indirectly through uptake of water in the vadose zone (Burt, 1979; Graham et al., 2013) (Figure 1b). Vadose-zone root water uptake during the day increases soil matric potential gradients, driving groundwater and unsaturated soil water toward the surface, and consequently decreases water flow toward the stream. At night, when ET is negligible, the water potential gradient between the subsurface and the atmosphere decreases, leading to an increase in lateral water flow toward the stream, and an increase in stream discharge.

More recently, Barnard et al. (2010) showed that upslope vegetation is important in the formation and evolution of diel fluctuations in lateral subsurface flow, and its relative importance is dictated by soil moisture. They found that the point of maximum coupling between ET and groundwater occurred after large-volume soil pore spaces drained, because there was direct competition for water within small pore spaces that was supplying both groundwater and transpiration. As soil moisture decreased, matric potential decreased, leading to a reduction in gravitationally drained water and a decoupling of hillslope soil moisture and streamflow. In this case, upslope vegetation can be responsible for the formation and evolution of diel signals in groundwater, but this connection is dictated by soil moisture. Moore et al. (2011) also argued that soil moisture mediates the connection between ET and streamflow. They found that correlations between transpiration and streamflow decreased progressively as soil moisture decreased and thus suggested that upslope tree water use, beyond the early dry season, was limited to vadose-zone water that was disconnected from the stream. The results of both Moore et al. (2011) and Barnard et al. (2010) may be consistent with the saturated wedge hypothesis when soils are moist; however, they both determined that as the hillslope soil dried, ET and baseflow become more decoupled, and thus the saturated wedge hypothesis may no longer be applicable. These findings suggested that mechanisms connecting ET and discharge may shift from being controlled by both hillslope and riparian mechanisms to solely riparian mechanisms with decreasing soil moisture.

Here, we test the riparian interception and saturated wedge hypotheses, recognizing that these hypotheses were formulated from a mostly hydrologic perspective, though it is likely that transpiration-driven diel fluctuations also depend on geological and ecological processes within the critical zone (CZ). The CZ—an open system extending from the top of the canopy to the base of groundwater—hosts the physical, chemical, and biological processes that support life (Brantley et al., 2017). Generally, there are three types of subsurface water reservoirs in the CZ that can be used by trees: unsaturated soil moisture, rock moisture (water stored in the unsaturated zone in weathered bedrock), and groundwater. Recent work has stressed the importance of rock moisture as an important water reservoir for trees during the growing season (Hahm et al., 2019; Klos et al., 2018; Rempe & Dietrich, 2018). Rock moisture may be poorly connected or completely disconnected from groundwater supplying the stream during the growing season but may serve as a reliable source of water for vegetation during summer drought conditions (Dralle et al., 2018). Tree roots of some species can span the entire depth of the CZ; however, the need to invest in roots at greater depths depends on the availability of resources in the shallow subsurface, while the ability to root at depth depends on the permeability of the subsurface (Brantley et al., 2017). To determine where diel fluctuations are generated, we need to know which of these water reservoirs tree roots access as well as when they rely on water from these reservoirs. Perhaps, as soil and rock moisture declines, rather than forest transpiration and baseflow becoming more decoupled as suggested by Barnard et al. (2010) and Moore et al. (2011), transpiration and baseflow could become more coupled because trees rely on deeper roots that access water that is more connected to baseflow.

We investigate the origin of diel signals in unsaturated soil water, groundwater, and streamflow from three hillslopes, systemically assessing how the diurnal signal in ET is propagated through the subsurface. Hillslopes were chosen based on differences in geomorphic properties, vegetation characteristics, and aspect. To assess the relative importance of near-stream and upslope vegetation, hillslope geology, and soil moisture on the presence and behavior of diel fluctuations in baseflow, and to test competing conceptual models of ET-groundwater connectivity on hillslopes with and without riparian vegetation, we designed a field plan that would enable independent investigation of each mechanism. We expected (1) in riparian areas where groundwater is in close proximity to the soil that transpiration-driven fluctuations in

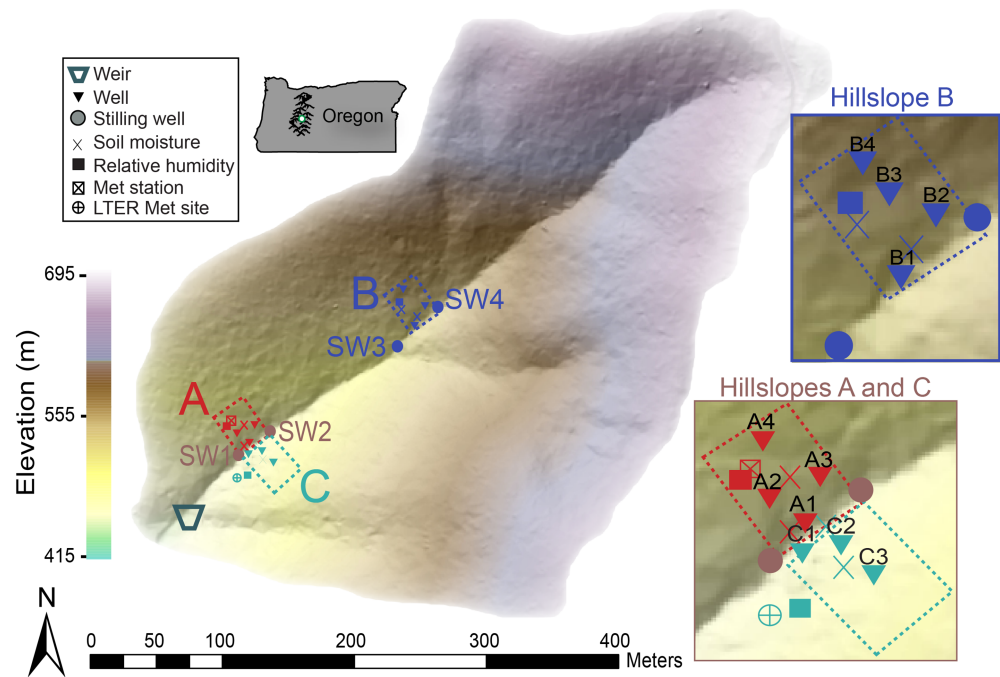


**Figure 2.** Location and overview of study area with outlines of the three investigated hillslope plots, including instrumentation, stilling well and the V-notch weir locations. The color scheme (red, blue, and turquoise) used to label each hillslope plot will be used in all following figures.

groundwater will be strongly correlated to transpiration and have large amplitudes; (2) when soil and rock moisture are high, forest transpiration and baseflow will be well coupled, but as soil and rock moisture declines, the two will become more decoupled due to decreasing unsaturated hydraulic conductivities; or alternatively, (3) as shallow moisture declines, forest transpiration and groundwater will be more coupled because trees will transition to the use of deeper water in the subsurface that is presumably more connected to groundwater.

## 2. Field Site

Our study site was Watershed 10 (WS10) of the H.J. Andrews Experimental Forest in western Oregon, USA. WS10 is a small 10.2-ha (0.1-km<sup>2</sup>) catchment (Figure 2) that has been the subject of extensive research on hillslope hydrology (e.g., Brooks et al., 2006; Brooks et al., 2010; Gabrielli et al., 2012; Harr et al., 1972; Harr, 1977; McDonnell et al., 2010; McGuire et al., 2007; Sollins et al., 1981; van Verseveld et al., 2009; Van Verseveld et al., 2017). WS10 was chosen because it has less-developed riparian areas at the lower end of the stream reach and more prevalent riparian areas in the upper reach as a result of multiple debris flows that removed near-stream soils and riparian vegetation (Graham et al., 2013), as well as unique, existing infrastructure. Hillslopes with (1) a slope break and a soil bench deposited in the near-stream area and (2) species common to riparian areas were considered to have a well-developed riparian area.

WS10 was initially established as a study basin to investigate changes in surface processes following a clear-cut harvest that took place in 1975. It is currently dominated by ~40-year-old Douglas-fir (*Pseudotsuga menziesii*) and sparse western hemlocks (*Tsuga heterophylla*) (McGuire et al., 2007). Bigleaf maple (*Acer macrophyllum*) and red alder (*Alnus rubra*) are common in the riparian areas (Graham et al., 2013). The understory vegetation is dominated by mostly shallow-rooted species: Oregon grape (*Berberis nervosa*), suppressed western hemlock trees, and huckleberry (*Vaccinium* spp.) (Brooks et al., 2006). The elevation of WS10 ranges from 450 to 680 m above mean sea level. The topography is characteristic of a V-shaped valley, defined by steep mountain hillslopes. The climate is Mediterranean, with dry summers and rain-dominated winters. The mean annual precipitation over the past 30 years is 2,180 mm with ~82% of this precipitation falling between October and April (PRISM Climate Group, 2017). The bedrock is composed of

**Table 1**  
*Comparison of Hillslope Characteristics on Slopes A, B, and, C*

| Hillslope characteristics                              |         |                  |                  |
|--|---------|------------------|------------------|
| Property   | Slope A | Slope B          | Slope C          |
| Distance upstream from the weir (m)                    | 91      | 250              | 86               |
| Near-stream slope                                      | 40°     | 31° <sup>a</sup> | 39°              |
| Slope length (m)                                       | 98      | 99               | 223              |
| Change in elevation (m)                                | 57      | 53               | 158              |
| Aspect   | South   | South            | Northwest        |
| Avg. near-stream soil thickness (m)                    | 0.1     | 1.9              | 0.1 <sup>b</sup> |
| Avg. upslope soil thickness (m)                        | 1.5     | >3 <sup>c</sup>  | >3 <sup>c</sup>  |
| Riparian area development                              | Poor    | Moderate         | Poor             |
| Avg. depth to near-stream groundwater through time (m) | 2.3     | 2                | 2.5              |

*Note.* Soil thicknesses were determined at well locations during drilling. Evidence considered to assess the degree of development of the riparian area (area within 5-m upslope of the stream) was (1) the vegetation composition and abundance and (2) if soil deposition on the valley floor formed a bench. Horizontal distances between the stream and near-stream wells were: 4 m in A1, 2.5 m in B1, and 2 m in C1 (Figure 3b). <sup>a</sup>3-m wide riparian bench present at base of hillslope. <sup>b</sup>Immediately increased to a thickness of ~1.75 m 0.5-m upslope from the stream. <sup>c</sup>Saprolite with a low penetration resistance may have been interpreted as soil in the upslope areas of hillslopes B and C; thus soils thickness in these areas may be closer to the 1.5 m reported by Harr (1977) on hillslope A.

forest density (Figure 3, Table 1). Harr (1977) classified the soil properties at nine different soil pits in the upslope area of hillslope A and found that the maximum soil depth was 1.5 m. Gabrielli et al. (2012) installed seven wells into the bedrock on hillslope A, four of which were monitored over this study. From here on these wells are referred to as A1, A2, A3, and A4 (corresponding to Gabrielli's wells A, B2, B3, and D) (Figure 2). Gabrielli et al. (2012) reported two distinct layers in the bedrock competency on hillslope A: a highly fractured and weathered layer that was approximately 1-m thick and a less-weathered layer with discrete fractures and occasional deep fractures. Near the stream, the depth to unweathered bedrock ranges from 0.1 to 0.6 m and gradually increases to 3 to 8 m up hillslope (Van Verseveld et al., 2017). At the base of hillslope A, there is a 10-m long flume to capture lateral subsurface flow discharging to the stream channel (McGuire et al., 2007). Numerous basaltic and rhyolitic dike outcrops have been identified throughout the H.J. Andrews Experimental Forest; one of which was identified within the length of this flume (Swanson et al., 1975). This geology suggests that some of the captured water likely originates from groundwater moving through the fracture networks that are more prevalent along the intrusive dikes. The flume diverts water to a box outfitted with a 15° V-notch weir, which we refer to as the flume box. Debris flows that occurred in 1986 and 1996 removed the near-stream vegetation that was present on hillslope A (van Verseveld et al., 2009).

Hillslope B, located ~250-m upstream from the stream weir (Figure 2), was selected because of its moderately developed riparian area, including thick near-stream soils forming a small 2- to 3-m wide terrace at the base of the hillslope and more-dense near-stream vegetation (Figure 3b, Table 1). Four wells were drilled on hillslope B (wells B1–4; Figure 2) using a Shaw Backpack Drill (<http://www.backpackdrill.com>). To isolate all bedrock wells from overlying soil water, bentonite seals were installed at the soil-bedrock horizon. The two distinct layers in the bedrock competency identified by Gabrielli et al. (2012) on hillslope A were also identified on hillslope B. Approximate soil depths on hillslope B were determined through our drilling campaign and a cone penetrometer survey—used to classify soils using resistance to penetration measurements—conducted on the H. J. Andrews Permanent Sample Plot network (<https://andrewsforest.oregonstate.edu/research/infrastructure/permanent-vegetation-plots>). Additional details on the cone penetrometer surveys in the H. J. Andrews and how they were used to determine soil depth can be found in Shanley et al. (2003). Recorded soil thicknesses were greater than the probe length of 3.05 m in the upslope area of hillslope B. Saprolite, with a low penetration resistance, may have been interpreted as soils in the cone penetrometer investigations. The primary characteristics

coarse breccia and andesitic and dacitic tuffs (Swanson et al., 1975). Above the consolidated bedrock lies saprolite, which may be as thick as 7 m (Gabrielli et al., 2012); however, the saprolite is not spatially continuous throughout the watershed and is often not present near the stream where floods and/or mass wasting events may have removed it (Gabrielli et al., 2012; van Verseveld et al., 2009). Overlying these layers are two dominant soil types: Typic Hapludands and Andic Dystrudepts (Yano et al., 2005). The two soils range in texture from gravelly, silty clay loam to very gravelly clay loam (McGuire et al., 2007). The bedrock-incised, perennial, first-order stream is approximately 320 m in length. Stream discharge over the year ranges from a typical winter storm event that peaks at ~40 L s<sup>-1</sup> (34 mm day<sup>-1</sup>) to summer base-flows around 0.2 L s<sup>-1</sup> (0.2 mm day<sup>-1</sup>) (Brooks et al., 2010).

Hillslopes were chosen based on differences in geomorphic properties, vegetation characteristics, and aspect, described below. Identified hillslopes from here on will be referred to as hillslopes A, B, and C. Each study plot was approximately 750 m<sup>2</sup>, and hillslope characteristics are summarized in Table 1 and conceptualized in Figure 3. Across the three hillslopes, we monitored 11 groundwater wells and six soil moisture profiles from 2016 to 2017.

Hillslope A has a southern aspect (Figure 2) and is located 91-m upstream from the stream gauge. It was selected because of its existing infrastructure and data, lack of riparian area, and comparatively low

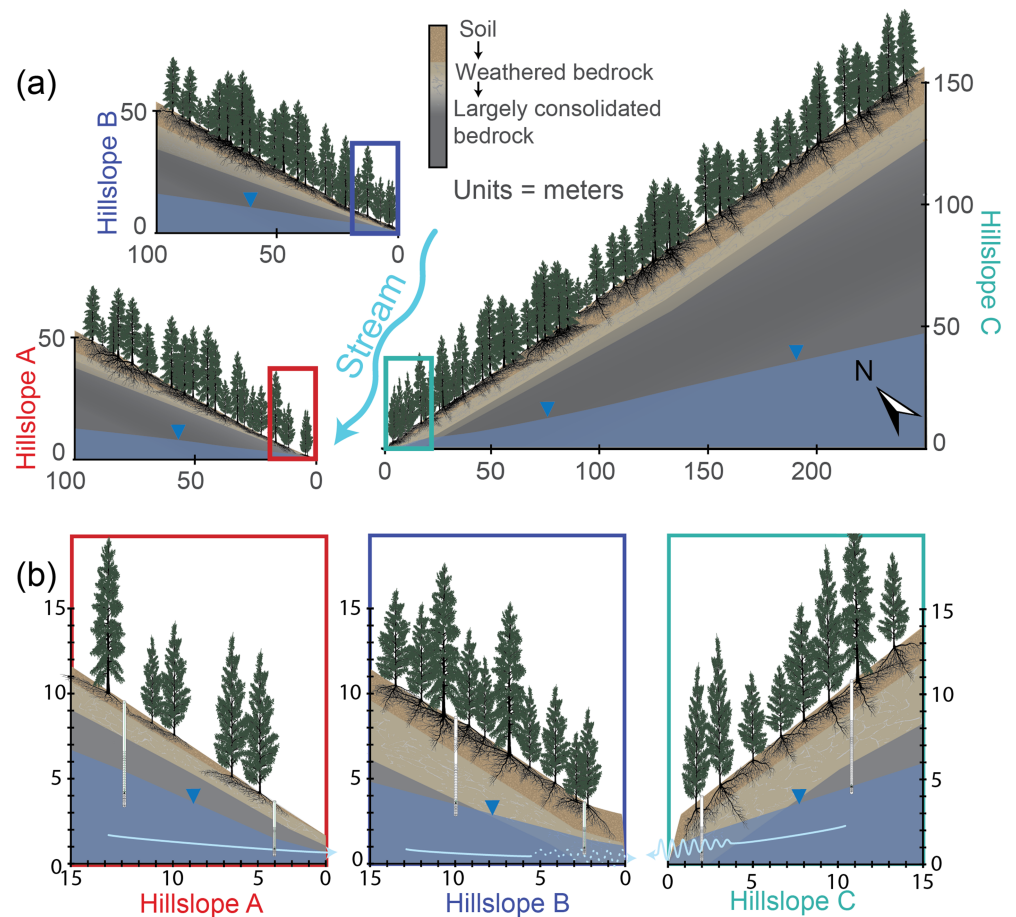


**Figure 3.** (a) Schematic hillslope cross sections. Thickness of units are approximate and inferred from limited subsurface data. Depicted root distributions are not based on field data but follow patterns commonly observed in Douglas-fir (Hermann & Lavender, 1990; Harrington et al., 2017). (b) Zoom-ins of near-stream areas. Light blue lines represent movement of the water table in near-stream areas. The light blue lines are dashed where diel fluctuations in groundwater were not consistent through time.

that distinguish hillslope B from hillslope A are greater near-stream vegetation density and thicker soils in the near- to mid-slope area.

Hillslope C has a northern aspect and is located directly across the stream from hillslope A. Hillslope C did not have a developed riparian area but had a greater density of near-stream and hillslope trees compared to hillslope A (Figure 3b, Table 1). Near-stream soil thickness increases to a depth of ~1.75 m within 0.5-m up hillslope A (Figure 3b, Table 1). Soil depth measurements determined with the cone penetrometer at the long-term vegetation plots upslope of hillslope C were greater than the 3.05 m probe length, but again, it is unclear if saprolite was interpreted as soils. Three bedrock wells—C1, C2, and C3—were drilled into the hillslope (Figure 2). The two distinct layers in the bedrock, identified by Gabrielli et al. (2012) on hillslope A, were also encountered during drilling on hillslope C.

The summer of 2017 was particularly dry, with approximately 5.8 cm of precipitation falling between June and July; the 30-year average during this time is 11.4 cm (PRISM Climate Group, 2017). The average daily temperature over this period was 1.5 °C higher than normal (PRISM Climate Group, 2017). Consequently, there were numerous long-duration fires in the region. Within a ~80-km radius around H.J. Andrews, a total of 404 km<sup>2</sup> burned between 10 August and 24 September (<https://www.fs.usda.gov/main/r6/fire-aviation>). Smoke from these fires may have had an effect on transpiration in WS10 and consequently influenced the physical and temporal characteristics of diel fluctuations in soil water, groundwater, and streamflow.

### 3. Methods

#### 3.1. Meteorological Measurements

Meteorological conditions were monitored on hillslope A (Figure 2). Net radiation, precipitation, relative humidity, air temperature, and wind speed and direction were recorded every 15 min on a Decagon Microclimate Monitoring System. A Campbell Scientific temperature and relative humidity sensor (083E-L) was installed 1.5 m above the ground surface on hillslope B and recorded data every 15 min on a Campbell Scientific data logger (CR1000). Understory air and soil temperature, and relative humidity (5-min intervals) were recorded approximately 20-m downstream of hillslope C at the H.J. Andrews Long-Term Ecological Research (LTER) (<https://andrewsforest.oregonstate.edu/data/streaming/other-stations/canopy-processes-hja-ecophysiological-and-microclimate-linkages>) climate station.

#### 3.2. Transpiration Estimates

Transpiration was estimated from sapflow measurements (i.e., xylem water flux) in 21 trees distributed over hillslopes A, B, and C. Instrumented trees were selected to be representative of the species and diameter distributions present on each hillslope. The sapflow data were recorded from 2 June through 14 September 2017 at 30-min intervals over the course of the growing season using the heat ratio method (Burgess et al., 2001). The measured heat-pulse velocity was converted into a sap flux velocity rate ( $\text{cm hr}^{-1}$ ) using the Barrett et al. (1995)-modified Marshall (1958) equation:

$$v_s = \frac{v_c \rho_b (c_w + m_c c_s)}{\rho_s c_s}, \quad (1)$$

where  $v_c$  is corrected heat-pulse velocity using Swanson and Whitfield (1981) method ( $\text{cm hr}^{-1}$ ),  $\rho_b$  is the density of wood ( $\text{kg cm}^{-3}$ ),  $c_w$  and  $c_s$  are specific heat capacity of the wood matrix and sap, respectively ( $\text{J kg}^{-1} \text{ }^\circ\text{C}$ ),  $m_c$  is the water content of the sapwood (unitless), and  $\rho_s$  is the density of water ( $\text{kg cm}^{-3}$ ). Values for these parameters were obtained from Miles and Smith (2009). Relative humidity data were used to calculate the vapor pressure deficit needed to set a baseline for nighttime sap flux data (Steppe et al., 2010). The calculated sap flux velocity,  $v_s$ , was used to determine a transpiration rate ( $\text{cm}^3 \text{ hr}^{-1}$ ) by multiplying sap flux velocity by the sapwood area. The sapwood thickness was determined by coring into the tree at breast height and then was used to calculate sapwood area.

#### 3.3. Soil Moisture, Soil Matric Potential, and Percent Loss in Root Hydraulic Conductivity

Soil volumetric water content (VWC) was measured at multiple near-stream (<3 m from stream) and mid-slope (>12 m from stream) locations on each hillslope. When soil thickness would accommodate, three Acclima TDT sensors (ACC-SEN-SDI) were installed at each location at depths of 30, 50, and 100 cm. Sensors were installed during the summer of 2015 and recorded data every 30 min over the 2016 and 2017 growing seasons. Acclima TDT sensors measured VWC (%), soil temperature ( $^\circ\text{C}$ ), bulk relative permittivity (unitless), and soil electrical conductivity ( $\text{dS m}^{-1}$ ). Acclima TDT sensors can resolve 0.06% changes in VWC; the typical absolute VWC accuracy is around 2% (<https://acclima.com/prodlit/UserManualSDITDT.pdf>). Because our primary concern is to assess relative changes in the timing and magnitude of diel fluctuations in soil moisture, we consider all diel fluctuations greater than the measurement resolution of these sensors (0.06%) to be viable. However, to improve the absolute accuracy of these soil moisture sensors, we calibrated them for soils in WS10 using the procedure described in Starr and Paltineanu (2002).

A peak in soil moisture in the morning hours, before transpiration has initiated, is a common observation in systems where trees show hydraulic redistribution, a process where roots move soil moisture laterally and/or vertically to water-depleted areas to protect against root hydraulic dysfunction (Richards & Caldwell, 1987). Diel changes in soil temperature can create a different pattern (a daytime maximum in soil moisture and a nighttime minimum) for sensors that use the electrical conductivity to estimate the VWC of a soil (e.g., Acclima TDT sensors). Electrical conductivity has a strong positive correlation with temperature increases. Diel changes in soil temperature were small (generally <2  $^\circ\text{C}$  at depths  $\leq 30$  cm) due to understory and overstory shading and thick layers of insulating duff, so we were minimally concerned about temperature strongly affecting soil moisture sensor data.

During our study period, soil matric potentials were measured using Tensiomark sensors (ecoTech, Bonn, Germany) at 15-min intervals on hillslope A at depths of 30 and 80 cm to determine relative water stress on tree roots (Voytek et al., 2019). The reported measurement accuracy for the tensiometers scales as  $\pm 5\%$  of the measured value (i.e., logarithm of pressure), with a minimum error of  $\pm 0.003$  MPa. Consequently, as the soil dries, error increases (i.e., at pressures less than  $-1$  MPa, there could be  $\geq 45\%$  error), so the data were compared to standard moisture release curves based on soil texture properties for WS10 by Ranken and Wesley (1974) (supporting information Figure S1), indicating that the measured values were reasonable. However, given the uncertainty in these data, we cannot statistically distinguish differences in matric potential data with depth. The Tensiomark data at 80-cm depth aligned best with the texture-derived moisture release curves, so we used the soil moisture and soil matric potential data at this depth to generate a retention curve to approximate soil matric potential at all soil moisture sensor locations over the study period.

The wilting point of trees is often much lower than the standard “crop plant” wilting point (e.g.,  $< -1.5$  MPa, Kramer & Boyer, 1995). Thus, it can be challenging to determine under what matric potentials tree hydraulic function may be jeopardized. To aid in our interpretation of how decreases in soil matric potential affect root hydraulic function and thus diel fluctuation generation, we calculated root water potentials using estimated soil matric potentials and the linear relation between these properties in Douglas-fir as developed by Domec et al. (2004). They also developed a vulnerability curve to predict the percent loss in root xylem conductivity (PLC) caused by xylem embolism over a range of soil matric potentials in young- (24 year) and old-growth (450 year) Douglas-fir tree roots. Domec et al. (2004) determined that the operating conductivity for Douglas-fir roots under moist conditions was between a PLC of 20 to 30, so PLC values over 30 were classified as “stressed.” We calculated the expected root PLC at varying soil depths as an indicator for root hydraulic stress and created three categories of stress: stressed, critical, and extreme. We categorized the root hydraulic stress as “critical” when soil matric potential was  $\leq -1.5$  MPa (crop plant wilting point) corresponding to root PLC  $> 52$ . Douglas-fir can take up water at water potentials below  $-1.5$  MPa (Brooks et al., 2006; Domec et al., 2004; Warren et al., 2005); however, we can expect that at more negative soil matric potentials normal root function would be jeopardized (e.g., limited root water uptake, increased root death, and a decrease in root regeneration; Domec et al., 2004). Estimated soil matric potentials become more negative than root water potentials at values less than  $-2.2$  MPa (corresponding to a PLC value of 70), which suggests that the normal root function is unlikely. Consequently, periods where daytime PLC values are greater than 70 were categorized as “extreme.”

### 3.4. Groundwater

Pressure head and groundwater temperature were measured using unvented U20-001-01 Onset™ pressure transducers (<http://www.onsetcomp.com/products/data-loggers/u20-001-01-ti>). Barometric pressure data were recorded on hillslopes B and C with U20 Onset™ pressure transducers placed  $>4$  m below the ground surface in a dry hole to monitor and correct for daily atmospheric temperature changes. Recorded pressure head measurements were then corrected for barometric effects using the HOBOWare Pro barometric compensation tool. This tool assumes fresh water and uses the transducer-measured temperature to account for changes in water density. After conversion from pressure head to water level, these sensors can estimate water level within error limits of  $\pm 0.4$  cm. This error includes effects of sensor drift, electronic noise, and temperature variations. Only three of the four wells had measurable water levels on hillslope A throughout the summer (A1, A2, and A3), as well as only two of four wells (B1 and B2) on hillslope B, and two of the three wells (C1 and C2) on hillslope C. The water level in the flume box weir on hillslope A was also monitored with a U20 pressure transducer to investigate if diel fluctuations in lateral subsurface flow (e.g., some combination of groundwater and throughflow) at a natural seepage face are markedly different than diel fluctuations in the water table.

Gabrielli et al. (2012) attempted pump tests in each of the groundwater wells they installed on hillslope A; however, the wells were pumped dry within 5–10 min at a discharge rate of  $< 0.1$  L  $\text{min}^{-1}$ . Pump tests were consequently not attempted in the wells installed during this field campaign; instead, all wells were injected with water at a rate of 20 L  $\text{min}^{-1}$  to assess aquifer properties.

### 3.5. Streamflow and Stage

Streamflow at the WS10 catchment outlet has been monitored since 1969. Since 1999, a large, low-angle, wet season weir is replaced each summer with a higher-angle V-notch plate weir to more accurately measure streamflow during low-flow conditions. The A Model 2 Stevens Instruments Position Analog Transmitter float-activated stilling well monitors stage at 5-min intervals, which is recalibrated for low-flow conditions in the summer. For water year 2017, streamflow data were obtained from the H.J. Andrews LTER gauging station network (<http://www.fsl.orst.edu/lter/>). Additionally, we installed four stilling wells (SW1, SW2, SW3, and SW4) above and below each studied hillslope (Figure 2): SW1 was installed 87 m above the WS10 gauge, SW2 at 120 m, SW3 at 275 m, and SW4 at 300 m. These stilling wells were installed to investigate the characteristics of diel fluctuations in streamflow. To secure the transducers and reduce noise due to turbulence, unvented U20 Onset™ U20-001-01 pressure transducers were installed into perforated PVC tubes that were drilled 0.5 m in the stream-incised bedrock. SW4 was installed in a particularly rocky and steep section of the stream, so sandbags were used to ensure that ample water would collect around the stilling well. Due to the rough nature of the stream bed and consistently low flows (approximately  $0.25 \text{ L s}^{-1}$ ), the stream could not be gauged at each stilling well location. Without a rating curve, the stilling well data could not be converted into a discharge; thus, analyses were performed with stream stage. To account for artificial pressure changes resulting from temperature changes that might be of similar magnitude to the variations in stage and flow we were exploring, the procedure suggested by Moore et al. (2016) was applied to each stilling well data set together with the HOBOWare Pro barometric compensation tool. This procedure enabled the development of a functional relation that could be used to post-correct pressure data for temperature.

### 3.6. Cross-Correlation

To determine the relation between time series data, the cross-correlation of sapflow—assumed to be the driver of diel signals in other data—and the other data showing diel cycling was calculated. We examined the time lag between sapflow and (1) groundwater, (2) soil moisture, and (3) stream stage and how lags changed through season. All data sets were interpolated to a 1-min resolution for the analysis. Cross-correlation analysis calculates two values: the correlation coefficient between two data sets and the time lag corresponding to that correlation coefficient. The lag corresponding to the point of maximum negative correlation was interpreted as the time offset (e.g., phase lag) between the peak in the transpiration signal and the minima in the signal in the compared data set. Positive correlations between sapflow and diel signals in other data would indicate that changes in the other data are driving fluctuations in sapflow, which we know to be unrealistic.

We developed an automated cross-correlation routine that calculated the cross-correlation between sapflow and another data set over a 3-day window at an incremental time step of 4 hr (i.e., the 3-day window is calculated at 0000 hr, again at 0400 hr, then at 0800 hr, etc.). Czikowsky and Fitzjarrald (2004) and Graham et al. (2013) determined that a 3-day time window was optimal because it was long enough to reduce the influence of storm events and short enough to capture diel signals between storm events. While there was little to no influence from storm events during our study period, we used 3-day windows to be consistent with previous literature. Changing the incremental time step within reason (i.e.,  $\pm 2$  hr) did not change the results. At each 4-hr time step, the Pearson correlation coefficient ( $r$ ) and the lag between sapflow and the other data set were calculated.

One complication in the lag analysis was that the diel signal in sapflow on many afternoons had no clearly distinguishable peak in mid-day due to variable cloud cover, local shading, other climatic factors, and/or modified stomatal-hydraulic conductance (e.g., Graham et al., 2013; McDowell et al., 2002) (Figure S2). To minimize the effects of these environmental and physiological factors on the cross-correlation calculations, all instrumented trees on each hillslope were averaged over each 3-day window in the cross-correlation routine and were then approximated with a sine wave:

$$y = A + B\sin(Cx + D) \quad (2)$$

where  $A$  is the offset above or below the axis about which the sine wave is oscillating,  $B$  is the amplitude,  $C$  is the frequency, and  $D$  is the phase shift in the sapflow data. To determine the frequency, a discrete Fourier transform that approximates discretely sampled data with a finite number of sinusoids was calculated using a fast Fourier transform (FFT). Peaks in the frequency-domain analysis corresponded to periodicities in the

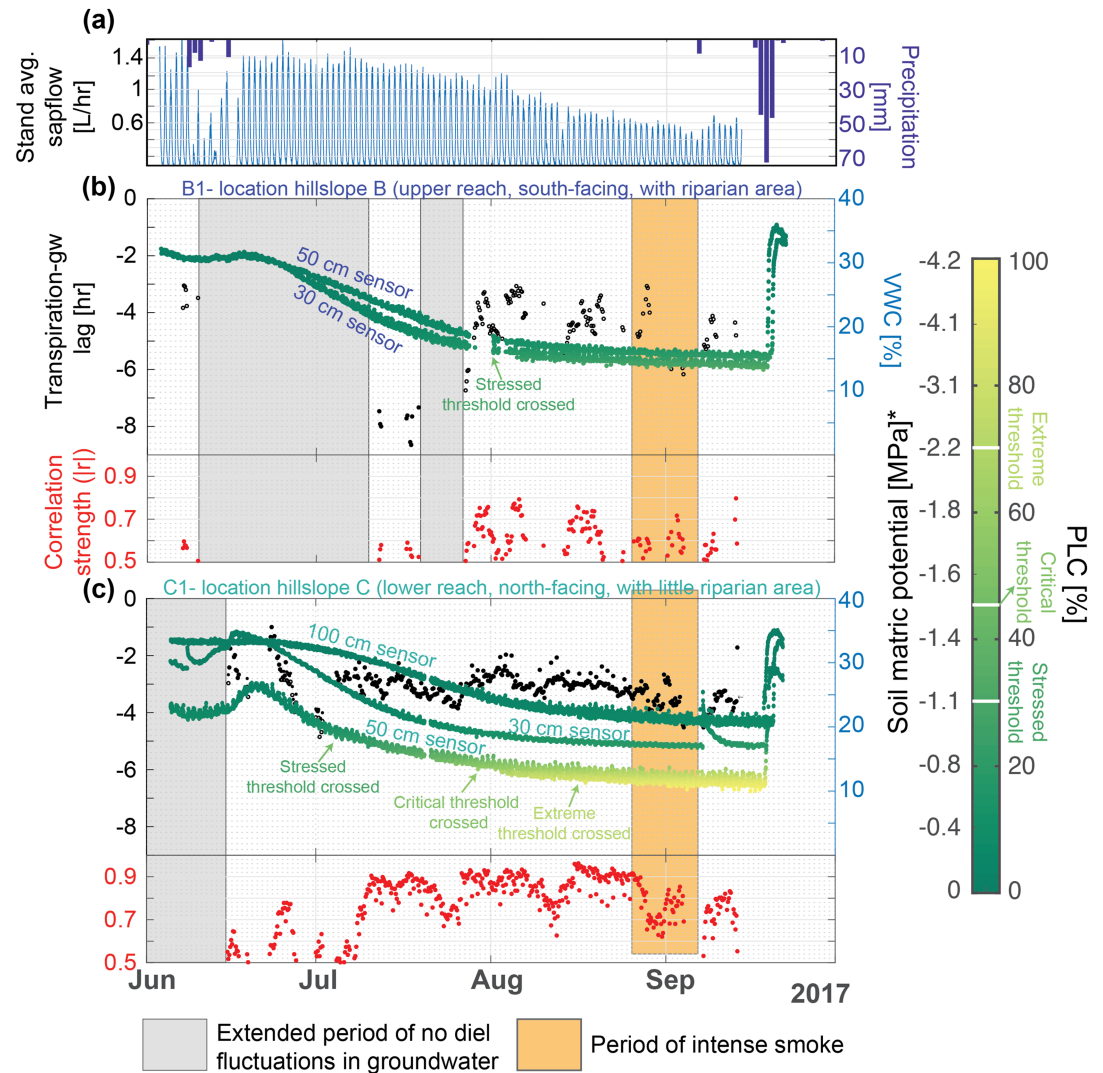


**Figure 4.** (a) Stand-average fluctuations in sapflow and daily total precipitation. (b, c) Lag (black dots) and the absolute value of the correlation strength (red dots) between sapflow and near-stream groundwater recorded in (b) B1, (c) and C1, with soil moisture content (VWC) at near-stream locations (plotted on the secondary y-axis). There were no diel fluctuations present in A1. Negative lags suggest that diel fluctuations in groundwater lag behind changes in transpiration (e.g., transpiration drives diel fluctuations in groundwater). Soil moisture color indicates the estimated soil matric potential and the predicted percent loss of root hydraulic conductivity (PLC) in the Douglas-fir assuming that roots have no access to rock moisture and groundwater. Soil matric potential tick marks are not equal due to the non-linear relationship between soil moisture and soil matric potential. Gray boxes indicate periods without diel fluctuations in groundwater.

data; as expected, the largest peak was observed at a frequency of 1/24 hr (or a period of 24 hr). The calculated frequency was then used in equation 2, and the other various coefficients were then determined through a nonlinear optimization routine yielding the best-fit sine wave approximation of the data. The correlation between the sine fit and the sap flow was always less than 0.5 on stormy days, when there were no diel fluctuations in the sapflow data. Thus, a correlation of 0.5 was used as a threshold to remove days with no transpiration from the cross-correlation analysis.

The groundwater and stream stage data went through three processing steps to isolate the diel fluctuations: (1) barometric pressure and temperature correction, (2) storm-event and seasonal-trend removal, and (3) a low-pass filter to remove random, high-frequency noise. Barometric and temperature corrections were discussed above. To remove both storm event and seasonal effects, the daily median groundwater and

**Table 2**

Change in VWC From 1 June to 17 September and Dates When Estimated Percent Loss in Root Conductivity (PLC) Surpassed Stressed (PLC > 30), Critical (PLC > 52), and Extreme (PLC > 70) Levels

| Depth                     | Dates of onset |                      |              | Absolute change<br>in VWC (%) | Median<br>VWC (%) | Maximum<br>VWC (%) | Minimum<br>VWC (%) |
|---------------------------|----------------|----------------------|--------------|-------------------------------|-------------------|--------------------|--------------------|
|                           | Stressed       | Critical             | Extreme      |                               |                   |                    |                    |
| Near-stream soil pits     |                |                      |              |                               |                   |                    |                    |
| Hillslope A               | 30             |                      |              | −13                           | 25                | 39                 | 18                 |
|                           | 50             | 19 July              |              | −11                           | 17                | 35                 | 13                 |
|                           | 80             | 28 July              |              | −15                           | 18                | 34                 | 13                 |
| Hillslope B               | 30             | 29 July <sup>a</sup> |              | −14                           | 21                | 37                 | 13                 |
|                           | 50             | 11 August            |              | −13                           | 22                | 36                 | 14                 |
| Hillslope C               | 30             |                      |              | −14                           | 20                | 35                 | 17                 |
|                           | 50             | 3 July               | 29 July      | −13                           | 13                | 30                 | 8                  |
|                           | 100            |                      | 16 August    | −14                           | 26                | 35                 | 20                 |
| Upper hillslope soil pits |                |                      |              |                               |                   |                    |                    |
| Hillslope A               | 30             |                      |              | −14                           | 27                | 41                 | 19                 |
|                           | 50             | 1 July               | 16 July      | −12                           | 12                | 28                 | 5                  |
|                           | 100            |                      | 26 July      | −11                           | 31                | 38                 | 25                 |
| Hillslope B               | 30             | 4 August             | 15 September | −17                           | 26                | 36                 | 12                 |
|                           | 50             | 24 July              | 29 August    | −17                           | 25                | 37                 | 11                 |
|                           | 100            | 10 September         |              | −19                           | 31                | 40                 | 16                 |
| Hillslope C               | 30             | 22 July              | 26 August    | −12                           | 16                | 36                 | 12                 |
|                           | 50             | 22 June              | 8 July       | −10                           | 14                | 30                 | 7                  |
|                           | 100            | Faulty sensor        |              |                               |                   |                    |                    |

<sup>a</sup>Date that could not be determined precisely due to data gaps.

streamflow elevations were calculated on each day over the study period, producing a time series of daily median values, per Graham et al. (2013). This time series was interpolated to 30-min time steps and then subtracted from the original time series, thus removing seasonal trends and storm events while leaving isolated diel fluctuations. High-frequency random noise on the order of 1–3 mm was apparent in all groundwater level and barometric pressure data sets. A dry (air-only) test of the pressure transducers produced 1–3 mm random noise, suggesting that this noise was likely due to instrument electronics. To reduce the influence of this noise, the water level data recorded in the field were processed with a low-pass filter in Matlab (scripts available; see acknowledgments section).

## 4. Results

### 4.1. Transpiration

Diel fluctuations in sapflow were observed throughout the study period except during an 8-day period of consistent precipitation and cloud cover that began on 8 June 2017. The average daily rate of maximum observed sapflow for all monitored trees was approximately 1.4 L hr<sup>−1</sup> in late June and decreased to 0.6 L hr<sup>−1</sup> in late August. For all monitored trees, there was little to no difference in the timing of sapflow (i.e., maximums and minimums in sapflow on each hillslope almost always occurred within ±1 hr of one another). There were two trends in the sapflow data over the data collection period: (1) a shift in transpiration timing during the day and (2) an overall decrease in the flux of water moving through the trees (Figure 4a). The start of transpiration shifted from 0600 to 0800 hr (Pacific Standard Time) over the course of the growing season, and the time at which transpiration ceases shifted from 2000 to 1830. The peak timing of sapflow calculated using the sine-approximated sapflow shifted from 1300 to 1400 hr.

### 4.2. Soil Moisture and Root Conductance

The shift from the wet to dry season, after the early- to mid-June storm events, was apparent in all soil moisture sensors (Figures 4b and 4c). In all soil moisture profiles, except for the near-stream soil moisture profile on hillslope B, the soils at 30-cm depth retained more water than the soils at 50 cm depth (Table 2). Soils at 100-cm depth also retained more water over the growing season than shallow soils.

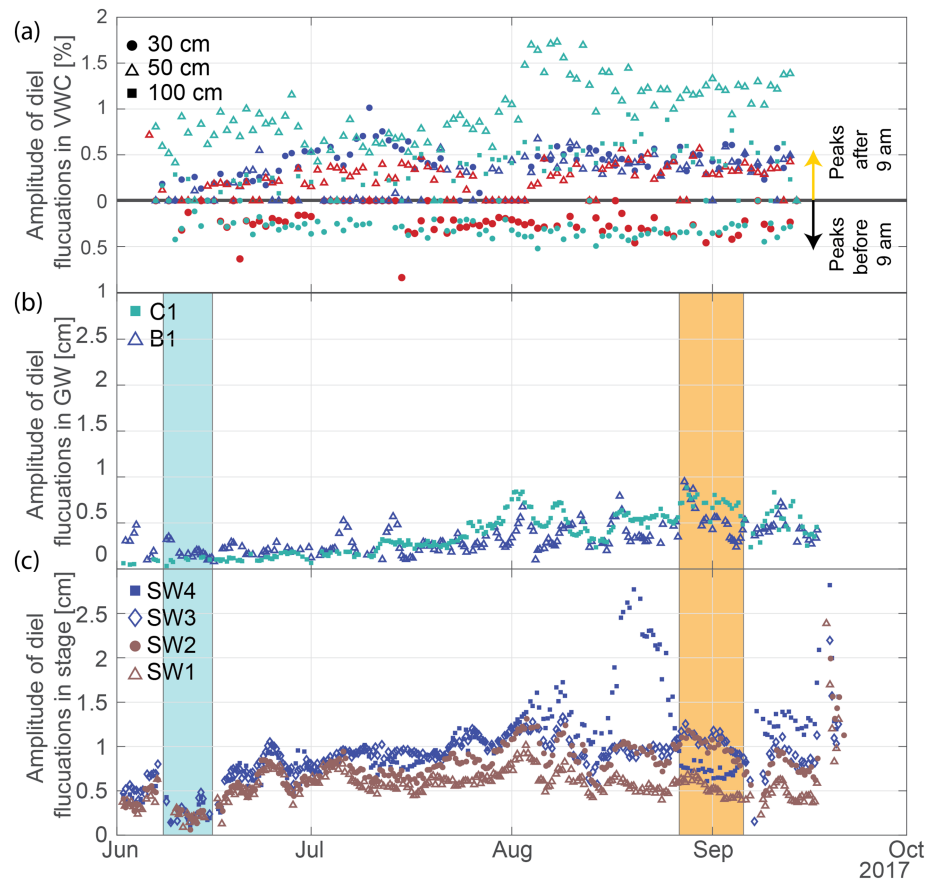


**Figure 5.** (a) Amplitudes of diel fluctuations in soil moisture (VWC). Markers above the zero line indicate that the peak VWC occurred after 0900 (most occur between 1300 and 1500), while markers below the line indicate that the peak in VWC occurred before 0900. Red symbols correspond to hillslope A, blue symbols to hillslope B, and turquoise symbols to hillslope C. (b) Amplitudes of transpiration-driven diel fluctuations in near-stream groundwater measured in B1 and C1; no diel fluctuations were observed in A1. (c) Amplitudes of diel fluctuations in stream stage measured in SW1–SW4 along the stream reach. The 8-day period of consistent cloud cover in June and the period of intense smoke in late August/early September that lead to decreases in amplitudes in diel fluctuations in groundwater and/or streamflow are highlighted by the light blue and orange boxes.

The maximum observed VWC was ~39%, recorded by the shallow, 30-cm sensor in the upper soil moisture profile on hillslope A. The observed minimum VWC was 8%, recorded in the 50-cm sensor at the upper soil moisture profile on hillslope C.

Diel fluctuations were apparent in all soil moisture sensors; however, the amplitude and phase of these fluctuations varied with depth, hillslope position, and among the three studied hillslopes. The magnitude of diel fluctuations in the 30-cm sensor on hillslope B over the summer was approximately 0.4%, while the amplitude in the corresponding sensors on hillslopes A and C were generally  $-0.22\%$  and  $-0.3\%$  (negative values indicate that peaks occur during the early morning). The diel fluctuations in soil moisture at 30-cm depth had peaks in VWC occurring before 0900 (except for the 30-cm sensor in the near-stream soil moisture profile on hillslope B; Figure 5a). In contrast to the other 30-cm sensors in near-stream locations, the peaks of the diel fluctuations in VWC observed at 30-cm depth in near-stream locations of hillslope B occurred during the afternoon (Figure 5a). The median amplitude of diel fluctuations was 0.92% in VWC in soils at 50-cm depth on hillslope C and was larger than the median amplitudes in the 100-cm (0.39%) and 30-cm ( $-0.3\%$ ) sensors (Figure 5a). The amplitudes in diel fluctuations in VWC on hillslope C increased as the summer progressed and were consistently larger than those observed on other hillslopes (Figure 5a).

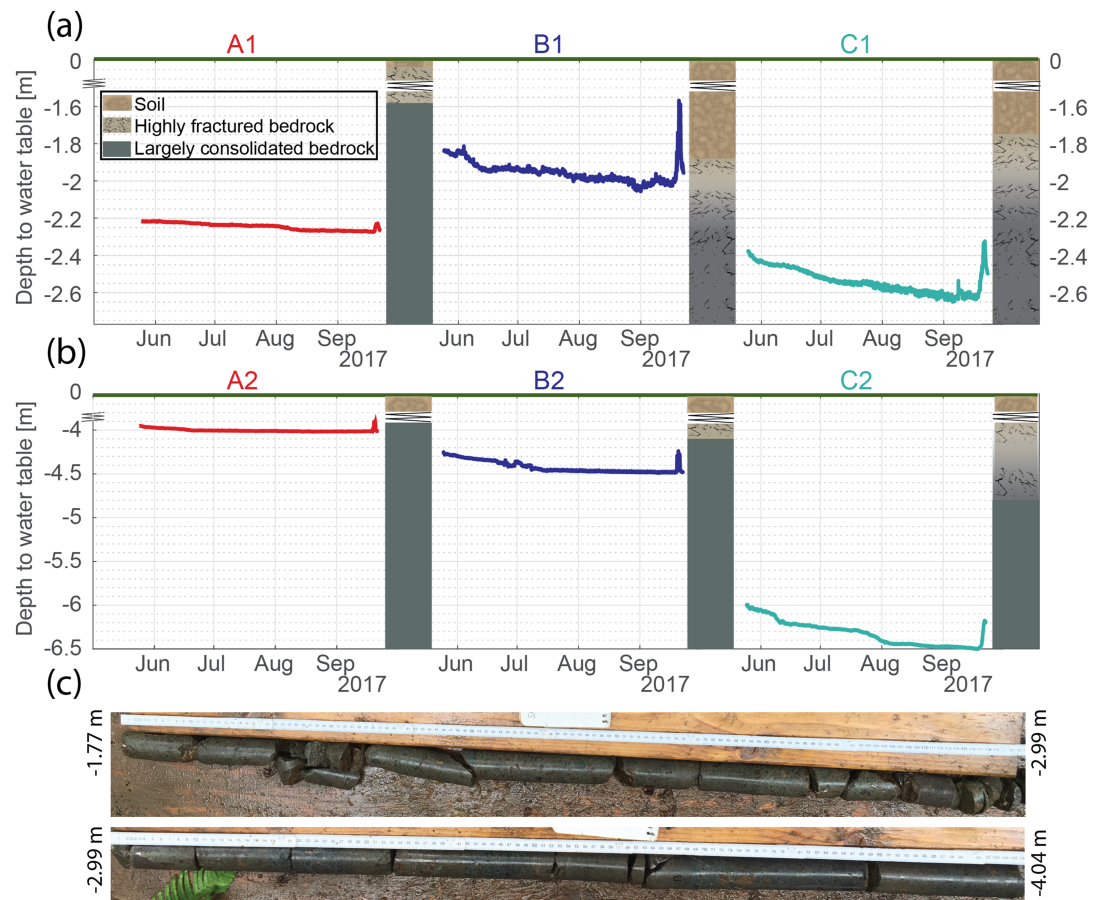


**Figure 6.** Groundwater recession in near-to-mid-slope wells, with lithologic logs superimposed. (a) Near-stream wells located <3 m upslope from stream, (b) midslope wells located 10–14 m upslope from stream, (c) images of the –1.77 to –4.04 m fractured bedrock section in well C1. The geology transitions from soil (light brown color), to heavily fractured bedrock (tan with fractures), and to largely consolidated bedrock (dark gray color).

Cross-correlations were performed between sapflow and soil moisture; however, because of the noise and the limited resolution of the soil moisture sensors, diel fluctuations in soil moisture would often look like a step pyramid. This shape led to highly variable cross-correlation results that could not be easily interpreted. For this reason, we do not discuss the results from these cross correlations.

### 4.3. Groundwater

Groundwater levels generally decreased from 24 May to 7 September 2017; however, there was considerable variability in water table dynamics measured on the three hillslopes (Figures 6a and 6b). Wells on hillslope A experienced a small head drop over the dry season relative to the other slopes; the water level at A1, A2, and A3 decreased of 5, 6, and 6.2 cm, respectively. Wells B1 and B2 decreased in water level by 18 and 22 cm over the dry season (Figures 6a and 6b). From late August through 7 September, there was an increase in the water level in B1 that does not correspond with precipitation but rather the period of intense smoke coverage that may have limited transpiration (Figure 6a). Wells intersecting the water table on hillslope C (C1 and C2) had the largest water table drop of any wells: a decrease of 48 cm in C2 and a decrease of 21 cm in C1 (Figures 6a and 6b). Two distinct periods of rapid reduction in water table height were observed in early June and mid-to-late July for C1 and C2.

The two wells drilled 16 and 23 m uphill from the stream on hillslope B (B4 and B3, respectively) were drilled 6.0-m and 6.1-m deep but did not intersect the water table at the time of installation. Water was observed in these wells after the large storm event in mid-September, but no diel fluctuations were observed. The

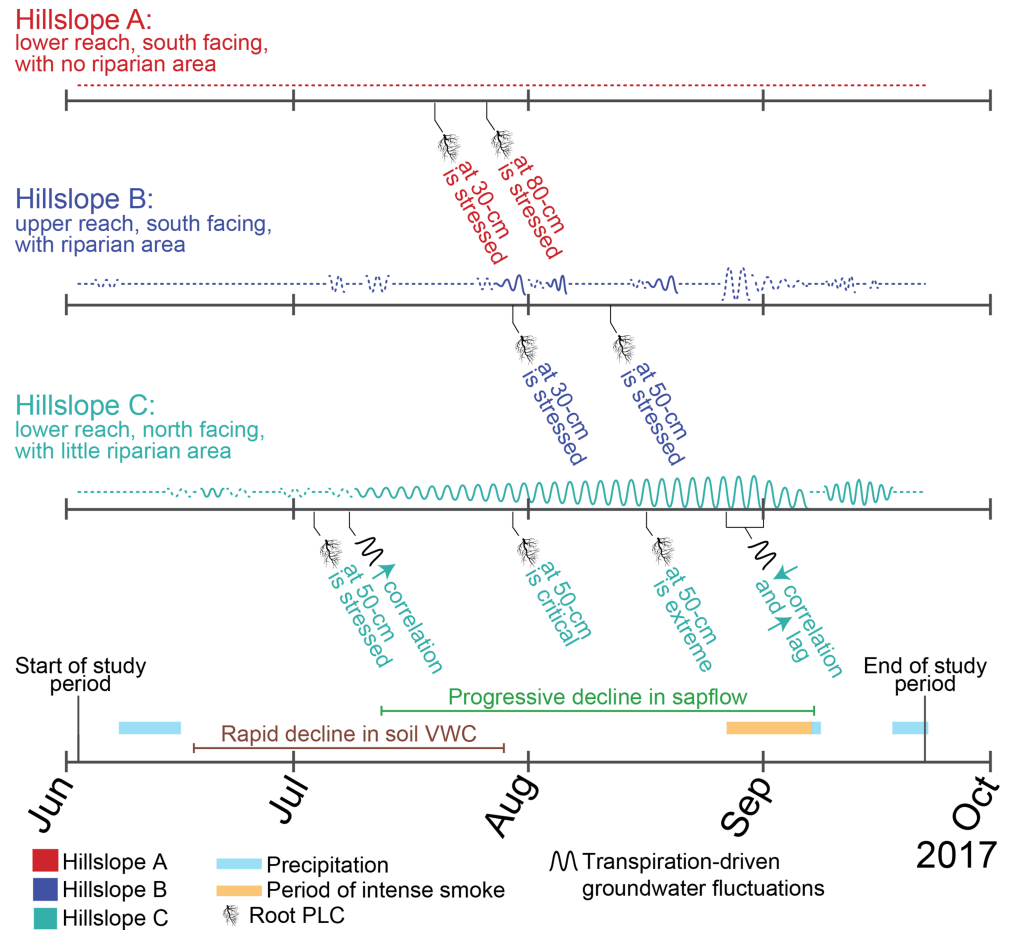


**Figure 7.** Timeline of important environmental events (e.g., precipitation and wildfire smoke) and transitions in tree-soil-groundwater connectivity in near-stream areas of the three studied hillslopes. Solid lined fluctuations indicate a strong correlation between transpiration and groundwater, while dashed lines indicated poor correlation.

uppermost well on hillslope C (C3) was the deepest well we installed at 8.2 m, yet also remained above groundwater for the entire study period. On hillslope A, the uppermost well A4, installed to a depth 7.8 m, also remained above groundwater for the entire study period.

Diel fluctuations were not observed in the groundwater wells on hillslope A. In A1, the water table resided in the largely consolidated bedrock, ~0.6-m below the zone of highly fractured bedrock, throughout the summer (Figure 6a). The only period of consistent diel fluctuations in the hillslope water flux diverted to the flume box was from 4–14 August. During this period, diel fluctuations had amplitudes <0.2 cm and were within the error limits of the HOBO U20 ( $\pm 0.4$  cm), so we are not confident that these fluctuations were real; consequently, cross correlation was not conducted between sapflow and the hillslope water flux.

The water level in well B1, drilled 2.5 m upslope from the stream, had consistent diel fluctuations beginning on 29 July, nearly the same time the roots at 30-cm depth passed the stressed PLC threshold (Figures 4b and 7). The correlation of these diel fluctuations with sapflow was greater than 0.7, and the calculated lag was ~4 hr ( $\pm 50$  min). However, over the period from early August to 17 September, there were day- to multi-day periods when there was no diel signal in groundwater or the signal was not greater than measurement error (Figures 4c and 7); the correlation with sapflow was also weaker during this time, ranging from 0.5 to 0.65. There was considerable seasonal variation in lag times (3–9 hr) and the corresponding correlation strengths in the water level fluctuations in B1; however, the amplitude of the fluctuations generally increased from 1 July to 17 September (Figure 5b).

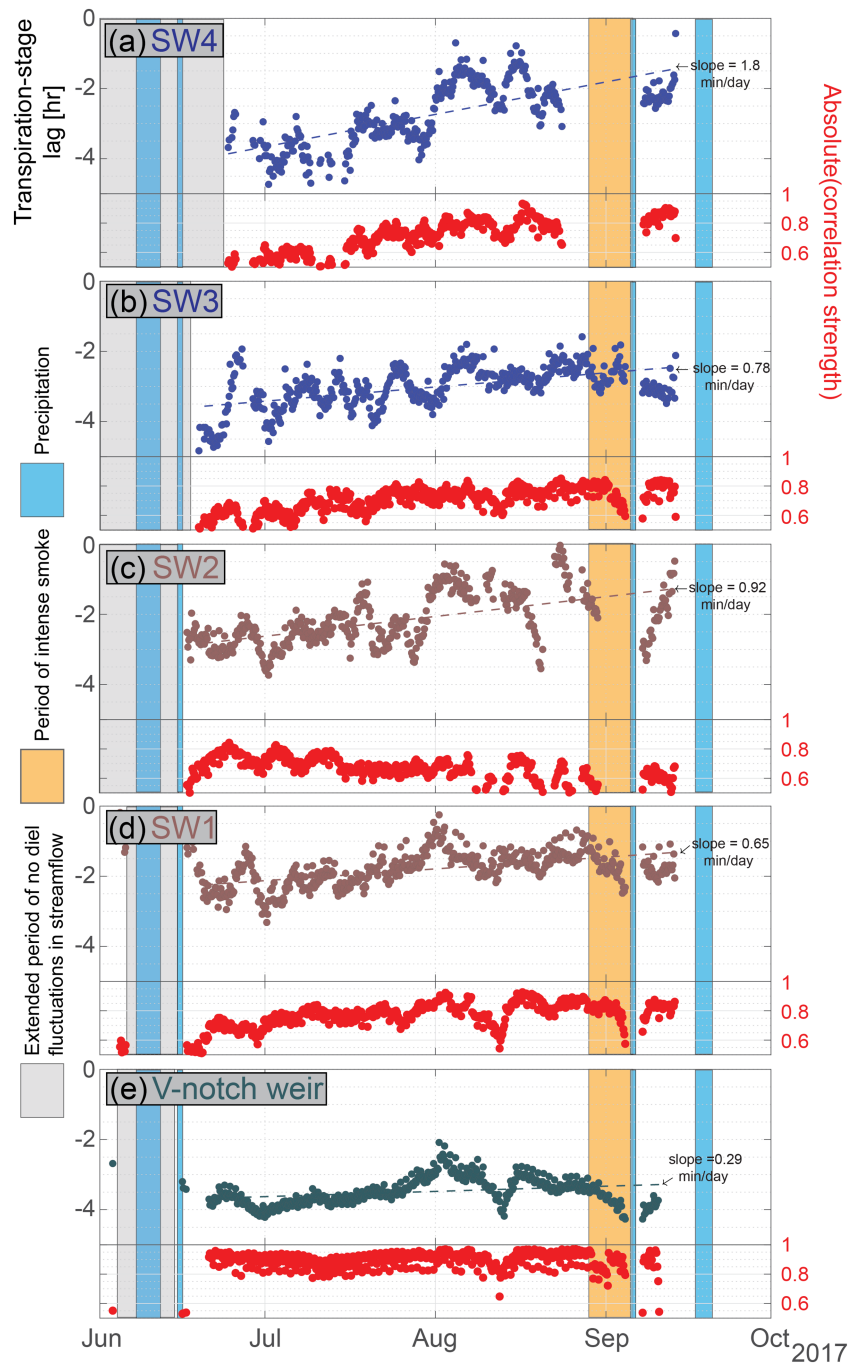


**Figure 8.** Lag and correlation strength between sapflow and stream stage at five different locations along WS10 stream reach from upstream (top) to downstream (bottom). Dots indicating lag times calculated in stilling wells near hillslope B are colored in blue, while the dots for stilling wells near hillslopes A and C are brown. Generally, lag times decrease while the correlation strength remains relatively constant. Gray boxes indicate periods without diel fluctuations in stream stage, blue boxes indicate storm events, and orange boxes indicate periods of high levels of smoke.

Diel groundwater level fluctuations were first observed in C1 on 17 June, approximately 1 month before diel diel fluctuations were noted in B1. At C1, the transpiration-driven diel fluctuations in groundwater were present before shallow soil moisture stores had been depleted (Figures 4c and 7), suggesting that a connection between deeper groundwater and transpiration existed before shallow soil moisture became limiting. In early July, the amplitude of transpiration-driven diel fluctuations in VWC increased and continued to do

so until the large storm event in mid-September (Figure 5b). From 23 July to 4 August there was a decrease in lag times from 4 to 2 hr, an increase in correlation strength from 0.7 to 0.92, and an increase in amplitudes of transpiration-driven diel fluctuations in near-stream groundwater from 0.25 to 0.82 cm (Figures 4c and 5b). By this time, soil moisture stores at 50 cm depth had been depleted, and the extreme PLC threshold was crossed (Figure 4c and Table 2).

#### 4.4. Streamflow

Stream stage, reported by all four stilling wells and the V-notch weir at the outlet of WS10, decreased from early June until late August, when a small increase is observed corresponding with the period of intense smoke from 24 August to early September (Figure S3). Discharge calculated using the V-notch weir decreased from  $\sim 3,000 \text{ L hr}^{-1}$  on 1 June to  $110 \text{ L hr}^{-1}$  on 1 September. Consistent, asymmetric, diel fluctuations in stream stage were observed for the entire period that the V-notch weir was in place (20 June to 15 September; Figures 8e and S3a). The asymmetric diel cycle in discharge, distinguished by the gradual rise and sharp decline in stage, is a common feature in many small watersheds in the summer months (Bond et al., 2002; Bren, 1997; Lundquist et al., 2002; Yashi et al., 1990).

Diel fluctuations in stream stage were observed from 17 June to 7 September in SW1, SW2, and SW3. There was a delay in the first appearance of diel fluctuations with increasing distance upstream. Diel fluctuations were first observed in SW1 and SW2, followed by SW3 three days later and SW4 one week later. Lag times between transpiration and stream stage increase in all stilling wells over the summer and were shorter with increasing distance downstream (Figure 8). In SW4, diel fluctuations were not observed continuously over the study period. On 16 August, amplitudes of diel fluctuations in SW4 increase rapidly from 1.2 to 3 cm and lag times increased from 1.2 to 3 hr. From 19 August to 7 September, there were no observable diel fluctuations in SW4, but they were observed again after the 7 September storm event. The sudden disappearance of diel fluctuations from 19 August to 7 September may be explained by the period of minimal transpiration due to smoke. Over this period, the water level recorded in SW4 increased by  $\sim 1$  cm.

## 5. Discussion

### 5.1. The Influence of Hydrogeologic Heterogeneity on Diel Fluctuations

#### 5.1.1. In Upslope Areas

We did not see evidence of diel cycles in the upslope groundwater data for any of the hillslopes where we had data, likely due to the depth of water table and the low unsaturated hydraulic conductivity of the bedrock. The water table recorded in wells a few meters upslope of the stream ranged from 4 to 6.5 m deep (Figure 6b). During water injection tests, the zone of highly fractured bedrock easily accommodated the  $20 \text{ L min}^{-1}$  of added water (there was no backflow observed in the well casing), suggesting ample storage capacity and/or high hydraulic conductivities. These results appear contradictory to low storage capacity and/or low hydraulic conductivity observed during the pump test by Gabrielli et al. (2012); however, the structure of the bedrock could allow both of these results to be true. The pump tests of Gabrielli et al. (2012) were conducted in bedrock with few fractures and a low hydraulic conductivity, whereas we injected water into a shallower layer of high hydraulic conductivity bedrock. While this fractured bedrock has a high saturated hydraulic conductivity, it is likely that it has a low unsaturated hydraulic conductivity. We hypothesize that the low unsaturated hydraulic conductivity of this highly fractured bedrock, which lies above the groundwater table in these wells, severed hydraulic connection between the groundwater table and rock and soil moisture. Because the water table resided within the largely consolidated bedrock and the unsaturated, highly fractured bedrock effectively separated soil water and groundwater in upslope areas, a strong transpiration-groundwater connection did not exist on the three hillslopes we studied. While the saturated wedge hypothesis thus did not explain our data, it may be relevant on hillslopes where the geology does not sever the connection between soil water and groundwater. In Barnard et al.'s (2010) 24-day irrigation experiment, transpiration-driven diel groundwater fluctuations were observed in the flume box at the base of hillslope A. However, these diel fluctuations may have only existed because of the wet conditions induced by the sprinkler experiment, which likely increased connectivity between draining soil water and groundwater. The strong connection between soil moisture and streamflow uncovered in Moore et al.'s (2011) findings in WS2 of the H.J. Andrews Experimental Forest may also suggest that the saturated wedge could apply during moist unsaturated zone conditions.

We looked to explore whether trees would transition to groundwater as shallow moisture stores decrease in upslope areas. Evidence of hydraulic redistribution in upslope soils (e.g., increases in shallow soil moisture during the night and decreases throughout the day) may suggest that deeper subsurface water was increasingly used as the summer progressed (Brooks et al., 2002). Root water stress in upslope shallow soils (<50 cm depth) increased at a faster rate than soils at the same depth in near-stream areas (Table 2). Because of limited deep subsurface data in upslope areas, including a lack of rock moisture measurements, we do not have direct evidence that can tie tree water use to a specific depth and can only hypothesize using the information available. The root morphology of Douglas-fir is controlled by soil and bedrock properties (Hermann & Lavender, 1990). While most of the root mass is found in the disaggregated material above bedrock, fine roots and larger structural roots can penetrate tens of meters into bedrock when fractures are present (e.g., Canadell et al., 1996; Estrada-Medina et al., 2013; Hasselquist et al., 2010; Poot et al., 2012; Witty et al., 2003). If roots were in direct contact with water table and were actively redistributing groundwater to shallow soils, then transpiration-driven fluctuations should have propagated through groundwater and been evident in groundwater levels a few meters upslope of the stream. If trees in our upslope areas relied on rock moisture, and this water was disconnected from groundwater, then it would not be surprising that we did not see evidence of diel fluctuations in groundwater wells upslope of near-stream areas.

### 5.1.2. In Near-Stream Areas

Without explicit knowledge of where near-stream trees were rooted and where they accessed water, we cannot determine if diel fluctuations in groundwater result from tree water uptake that was soil moisture mediated or from direct uptake of groundwater. However, the depth to the groundwater table and the geology at that depth likely dictated rooting depth and controlled where and when the transpiration-driven diel fluctuations were apparent in riparian groundwater. Hillslopes B and C were selected without prior knowledge of the water table depth. Data were available on hillslope A during the wet season when transpiration is limited (Gabrielli et al., 2012). After installation of near-stream groundwater wells on hillslopes B and C, we found that the groundwater was shallowest in B1 at ~2 m depth, followed by A1 at ~2.3 m depth, and C1 at ~2.5 m depth (Figure 6a). The difference in depth to groundwater in these near-stream areas was unlikely to be large enough to drive the variability in the diel fluctuations observed in groundwater on the three hillslopes (Figure 3b). However, differences in bedrock properties where groundwater resides may be important enough to have driven the differences in groundwater patterns.

We hypothesize that the primary reason why transpiration-driven fluctuations in near-stream groundwater were not observed in A1 is that groundwater resided within the zone of largely consolidated bedrock, where substantial root growth was unlikely (Figure 6a). In B1 and C1, the water table resided within the zone of highly fractured, permeable bedrock, where root growth is possible (Figure 6a). We expected that because hillslope B had a well-defined riparian area, there would be a strong ET-driven signal in B1, whereas there would be a weaker signal in C1 given its less well-defined area. Contrary to our expectations, a stronger ET signal was observed in groundwater in C1 than B1. In comparison to B1, transpiration-driven diel fluctuations in C1 (1) appeared earlier in the growing season; (2) were more persistent throughout the growing season; (3) had larger amplitudes; and (4) were more strongly correlated to transpiration (Figures 4b and 4c). These results point to the presence of roots with direct access to groundwater and the applicability of the riparian interception hypothesis. In C1, the water table and soils were separated by a zone ~80 cm thick of highly fractured (i.e., more accessible to root penetration) unsaturated bedrock. The low unsaturated hydraulic conductivity of this zone of bedrock fractures would suggest that transpiration-driven diel fluctuations in groundwater were not caused by water potential gradients in the soil above but were more likely the result of trees rooting to the water table.

Transpiration-driven groundwater fluctuations in B1 (1) were not observed every day, (2) were apparent later in the season than C1, (3) had smaller amplitudes than those observed in C1, (4) were less correlated (ranged from 0.5 to 0.8) than those observed in C1, and (5) had lag times that were generally greater than 3 hr (Figures 4b, 4c, and 5b). By mid-June, the groundwater table was located 5 cm below the soil-bedrock interface in B1, and it remained within 15 cm of this interface until the 17 September rain event when it rose (Figure 6a). Compared to hillslopes A and C, there was little difference between the 30- and 50-cm soil-moisture sensors throughout the study period on hillslope B, and soils at 50 cm depth retained more moisture in comparison to near-stream soils on hillslope C (Figures 3b and 3c and Table 2). The close proximity of the soil-bedrock interface to the water table may have allowed for easier redistribution of

groundwater via roots and/or soil moisture gradients. Similar observations were made by Barbeta and Peñuelas (2017) and Fan et al. (2017), who found that root depth and root function (e.g., water uptake) varied spatially as a function of depth to the water table, and in cases where the groundwater table was in contact with soil, tree groundwater use was mediated by soil moisture.

Stable soil moisture conditions may explain the weaker correlations between transpiration and groundwater in B1, including the delay in the appearance of transpiration-driven diel fluctuations. Hasenmueller et al. (2017) observed that tree-root densities in fractures were significantly lower in toe-slope locations in comparison to upslope locations in a Pennsylvania forest situated on shale, despite increased fracture density in toe-slope locations. They reasoned that because the water table is shallow in toe-slope locations, there was less of a need to increase root growth at depth. The close proximity of the water table to the soil-weathered bedrock boundary on hillslope B as the dry season progressed (within 5–15 cm) likely led to high soil moisture availability for trees, suggesting that trees may not need to invest in deeper roots within bedrock fractures. Wet soil conditions may also explain why there was no evidence of hydraulic redistribution in these near-stream soils on hillslope B, even after roots at <30 cm depth were stressed. Perhaps the majority of roots in this near-stream area were at depths greater than 30 cm where both soil water and essential nutrients were available.

The difference in lag times between C1 and B1 alone does not seem large enough to suggest that transpiration is less connected to groundwater on hillslope B than on hillslope C. However, the diel fluctuations in B1 were sporadic, and there were multi-day periods in the late summer when the correlation between transpiration and groundwater was less than 0.5 (Figures 4c and 7). It remains unclear why these periods of poor connection between transpiration and groundwater existed on hillslope B; however, these periods would likely not exist if a large density of roots was in direct contact with the water table.

In short, results from near-stream wells suggest that the generation of transpiration-driven diel fluctuations is controlled by proximity of the water table to the base of the soils and permeability of the bedrock in the location where the groundwater resides. The lack of transpiration-driven fluctuations in groundwater on hillslope A suggests that when the water table resides at a depth where fractures are not conducive to root growth, groundwater and transpiration will be disconnected. When the water table was near the soil-bedrock interface as on hillslope B, root development in the fractured bedrock may not have been necessary, and the influence transpiration had on groundwater would be strongly dependent on soil moisture properties. In near-stream areas where the water table was well below the soil-bedrock interface but resided at a depth where numerous fractures enable root growth, transpiration and groundwater will be well connected and diel fluctuations will be prevalent. The spatial heterogeneity in near-stream hydrogeology controls diel-signal formation, and thus where trees pull water from may be unpredictable without subsurface knowledge.

## 5.2. Changes in Amplitude of Diel Fluctuations in Groundwater and Stream Stage

Over the 2017 summer, we observed that the amplitude of diel fluctuations in groundwater levels in B1 and C1 increased as soil water storage decreased (Figure 5b). Similarly, the amplitudes in diel fluctuations in stream stage increased (Figure 5c). However, during the 8-day period of consistent cloud cover in June and the period of intense smoke in late August, normal transpiration was limited, leading to a reduction in amplitudes of diel fluctuations in groundwater and/or stream stage and a decrease in correlation with ET (Figures 4b and 4c, 5b and 5c, and 8). Amplitudes of diel fluctuations in near-stream groundwater in B1 and C1 decreased by an average of 0.47 and 0.36 cm during the period of intense smoke. Amplitudes of diel fluctuations in all stilling wells diminished by an average of 0.36 cm during the period of cloud cover and by an average of 0.6 cm during the period of intense smoke. These periods of decreased amplitudes and correlation provide additional evidence that ET controlled diel fluctuations in groundwater and streamflow. In the near-stream area of hillslope C, where roots were likely in direct contact with groundwater, hydraulic redistribution of groundwater to soils at 30 cm depth likely occurred throughout the summer (Figure 6a). Amplitudes of diel fluctuations in water level in C1 increased in early July when roots at 50 cm crossed the stressed threshold, suggesting that as deeper soil reserves dry more groundwater was needed to protect against hydraulic dysfunction in roots less than 30 cm (Figure 5c and Table 2).

Wondzell et al. (2010) also observed increases in amplitude of diel fluctuations in near-stream groundwater as the summer progressed. They argued that in the early summer, ET demands were met with soil water, leading to small amplitudes in diel groundwater fluctuations. As the soil dried, ET demands were transmitted more directly to the groundwater aquifer through a steeper soil matric potential gradient, leading to larger amplitudes in diel groundwater fluctuations. Similarly, we saw as the unsaturated zone dried, amplitudes in diel fluctuations increased in B1 (Figure 5b). However, another consequence of decreasing moisture is that the unsaturated hydraulic conductivity should decrease, which could lead to the decoupling of groundwater and transpiration, as suggested by Moore et al. (2011) and Barnard et al. (2010). Amplitudes of diel fluctuations in groundwater increase through the summer, which would seem to suggest increased coupling between groundwater and transpiration, but many of these fluctuations were poorly correlated with transpiration. It remains unclear why these periods of poor connection between transpiration and groundwater existed on hillslope B; it is possible that there is destructive interference between local transpiration from riparian groundwater and transmission of signals from upstream in the channel network that also impact the local groundwater elevation.

The amplitudes of temperature-corrected diel fluctuations in the stream are larger than diel fluctuations in groundwater (Figures 5b and 5c). This observation leads to another question: Are fluctuations in near-stream groundwater caused by transpiration in near-stream areas or can fluctuations in stream stage propagate upgradient and contribute to fluctuations in near-stream groundwater? If diel fluctuations in the stream propagated upgradient, we would expect to see fluctuations in all near-stream groundwater wells. Diel fluctuations were not present in groundwater levels in A1, and in B1 diel fluctuations were sporadic, suggesting that the consistent fluctuations in the stream are not fully driving fluctuations in riparian groundwater.

## 6. Conclusions

This study was designed to assess near-stream and upslope controls on the formation and propagation of transpiration signals. Our results revealed that the formation of diel fluctuations in groundwater was limited to near-stream areas. We had expected that in the early summer, when soil and rock moisture were high, diel fluctuations would be present in upslope groundwater because higher effective hydraulic conductivities would increase connectivity between the rhizosphere and groundwater; however, there were no diel fluctuations in wells upslope of near-stream areas. We hypothesize that the absence of diel fluctuations in upslope groundwater is because (1) root-groundwater contact is unlikely given that the water table resides within the largely consolidated bedrock and (2) the low unsaturated hydraulic conductivity of the fractured bedrock above the water table severs the connection between groundwater and transpiration. This hypothesis suggests that upslope tree water use in watershed 10 is met by soil moisture and rock moisture; however, we do not have direct measurements of the latter in this study. Direct measurements of rock moisture would help test our hypotheses above by constraining hydrologic connectivity between subsurface reservoirs in space and time.

In near-stream areas, we hypothesized that the close proximity of groundwater to soils would lead to consistent and strongly correlated transpiration-driven fluctuations in groundwater throughout the growing season. However, diel fluctuations were not ubiquitous in space and time because bedrock permeability and the depth to the water table control whether roots will be in direct contact with groundwater. Based on our observations, we suggest that if the water table resides well below the soil-fractured bedrock interface—and the bedrock fractures can accommodate root growth—then trees will increasingly utilize groundwater as soil moisture stores are depleted and groundwater diel fluctuations will be evident. However, if the water table is in contact with soils, roots may not need to penetrate into fractures to access groundwater. Under these conditions, plant water uptake remains moisture mediated, and the presence of diel fluctuations in groundwater will depend on soil matric gradients and the hydraulic conductivity of the unsaturated zone.

In this study, we demonstrate that diel fluctuations can be used as a diagnostic tool to explore where and when trees use water within hillslopes. This tool provided evidence that the position of the water table and the structure of weathered bedrock—including its variations in hydraulic conductivity—controlled the connection between the saturated zone and the rhizosphere. These conclusions likely look different in

watersheds with different underlying geologies, but hopefully motivate additional measurements in other systems to continue to improve quantification of how hydrogeology mediates the connection between plants and subsurface water stores and explore what information on near-stream hydrogeology can be gathered from diel fluctuations observed in streams.

### Acknowledgments

This research was supported by the National Science Foundation under Grants EAR-1446161 and EAR-1446231. We thank Jackie Randell, Daphne Szutu, Stephanie Jarvis, Benjamin Fahy, Emily Voytek, Megan Doughty, Ariel Rickel, and James Schaftenaar for field assistance; Chris Gabrielli for providing well information/access on hillslope A; Soutir Bandyopadhyay for discussions on time series analysis, and Stephanie and Jackie for sapflow calculations and water level processing. Data and facilities were provided by the H.J. Andrews Experimental Forest and Long-Term Ecological Research program, administered cooperatively by the USDA Forest Service Pacific Northwest Research Station, Oregon State University, and the Willamette National Forest. This material is based upon work supported by the National Science Foundation under Grant DEB-1440409. Data have been submitted to CUAHSI's Hydroshare (<http://www.hydroshare.org/resource/02e2e437a6044ea39bee0b95ec83fa1e>). <https://andrewsforest.oregonstate.edu/data>

### References

- Barbeta, A., & Peñuelas, J. (2017). Relative contribution of groundwater to plant transpiration estimated with stable isotopes. *Scientific Reports*, *7*(1), 10580.
- Barnard, H. R., Graham, C. B., Van Verseveld, W. J., Brooks, J. R., Bond, B. J., & McDonnell, J. J. (2010). Mechanistic assessment of hillslope transpiration controls of diel subsurface flow: A steady-state irrigation approach. *Ecohydrology*, *3*(2), 133–142. <https://doi.org/10.1002/eco.114>
- Barrett, D. J., Hatton, T. J., Ash, J. E., & Ball, M. C. (1995). Evaluation of the heat pulse velocity technique for measurement of sap flow in rainforest and eucalypt forest species of south-eastern Australia. *Plant, Cell & Environment*, *18*, 463–469. <https://doi.org/10.1111/j.1365-3040.1995.tb00381.x>
- Bond, B. J., Jones, J. A., Moore, G., Phillips, N., Post, D., & McDonnell, J. J. (2002). The zone of vegetation influence on baseflow revealed by diel patterns of streamflow and vegetation water use in a headwater basin. *Hydrological Processes*, *16*(8), 1671–1677. <https://doi.org/10.1002/hyp.5022>
- Brantley, S. L., Eissenstat, D. M., Marshall, J. A., Godsey, S. E., Balogh-Brunstad, Z., Karwan, D. L., et al. (2017). Reviews and syntheses: On the roles trees play in building and plumbing the critical zone. *Biogeosciences Discussions*, 1–41. <https://doi.org/10.5194/bg-2017-61>
- Bren, J. (1997). Effects of slope vegetation removal on the diurnal variations of a small mountain stream. *Water Resources Research*, *33*(2), 321–331.
- Brooks, J. R., Barnard, H. R., Coulombe, R., & McDonnell, J. J. (2010). Ecohydrologic separation of water between trees and streams in a Mediterranean climate. *Nature Geoscience*, *3*(2), 100–104. <https://doi.org/10.1038/ngeo722>
- Brooks, P. D., Chorover, J., Fan, Y., Godsey, S. E., Maxwell, R. M., McNamara, J. P., & Tague, C. (2015). Hydrological partitioning in the critical zone: Recent advances and opportunities for developing transferable understanding of water cycle dynamics. *Water Resources Research*, *51*, 6973–6987. <https://doi.org/10.1002/2015WR017039>
- Brooks, J. R., Meinzer, F. C., Coulombe, R., & Gregg, J. (2002). Hydraulic redistribution of soil water during summer drought in two contrasting Pacific Northwest coniferous forests. *Tree Physiology*, *22*(15–16), 1107–1117. <https://doi.org/10.1093/treephys/22.15-16.1107>
- Brooks, J. R., Meinzer, F. C., Warren, J. M., Domec, J. C., & Coulombe, R. (2006). Hydraulic redistribution in a Douglas-fir forest: Lessons from system manipulations. *Plant, Cell and Environment*, *29*(1), 138–150. <https://doi.org/10.1111/j.1365-3040.2005.01409.x>
- Burgess, S. S. O., Adams, M. A., Turner, N. C., Beverly, C. R., Ong, C. K., Khan, A. A. H., & Bleby, T. M. (2001). An improved heat pulse method to measure low and reverse rates of sap flow in woody plants. *Tree Physiology*, *21*(9), 589–598. <https://doi.org/10.1093/treephys/21.9.589>
- Burt, T. P. (1979). Diurnal variations in stream discharge and throughflow during a period of low flow. *Journal of Hydrology*, *41*(3–4), 291–301. [https://doi.org/10.1016/0022-1694\(79\)90067-2](https://doi.org/10.1016/0022-1694(79)90067-2)
- Canadell, J., Jackson, R. B., Ehleringer, J. B., Mooney, H. A., Sala, O. E., & Schulze, E.-D. (1996). Maximum rooting depth of vegetation types at the global scale. *Oecologia*, *108*(4), 583–595. <https://doi.org/10.1007/BF00329030>
- Constantz, J. (1998). Interaction between stream temperature, streamflow, and groundwater exchanges in alpine streams. *Water Resources Research*, *34*(7), 1609–1615.
- Constantz, J., & Zellweger, G. (1995). Relations between stream temperature discharge, and stream/groundwater interaction along several mountain streams.
- Czikowsky, M. J., & Fitzjarrald, D. R. (2004). Evidence of seasonal changes in evapotranspiration in eastern U.S. hydrological records. *Journal of Hydrometeorology*, *5*, 974–988. [https://doi.org/10.1175/1525-7541\(2004\)005<0974:EOSCIE>2.0.CO;2](https://doi.org/10.1175/1525-7541(2004)005<0974:EOSCIE>2.0.CO;2)
- Domec, J. C., Warren, J. M., Meinzer, F. C., Brooks, J. R., & Coulombe, R. (2004). Native root xylem embolism and stomatal closure in stands of Douglas-fir and ponderosa pine: Mitigation by hydraulic redistribution. *Oecologia*, *141*(1), 7–16. <https://doi.org/10.1007/s00442-004-1621-4>
- Dunford, E. G., & Fletcher, P. W. (1947). Effect of removal of stream-bank vegetation upon water yield. *Transactions, American Geophysical Union*, *28*(1), 105. <https://doi.org/10.1029/tr028i001p00105>
- Dralle, D. N., Hahm, W. J., Rempe, D. M., Karst, N. J., Thompson, S. E., & Dietrich, W. E. (2018). Quantification of the seasonal hillslope water storage that does not drive streamflow. *Hydrological Processes*. <https://doi.org/10.1002/hyp.11627>
- Estrada-Medina, H., Graham, R. C., Allen, M. F., Jiménez-Osornio, J. J., & Robles-Casolco, S. (2013). The importance of limestone bedrock and dissolution karst features on tree root distribution in northern Yucatán, México. *Plant and Soil*, *362*(1–2), 37–50. <https://doi.org/10.1007/s11104-012-1175-x>
- Fan, Y., Miguez-Macho, G., Jobbágy, E. G., Jackson, R. B., & Otero-Casal, C. (2017). Hydrologic regulation of plant rooting depth. *Proceedings of the National Academy of Sciences*, *114*(40), 10, 572–10,577. <https://doi.org/10.1073/pnas.1712381114>
- Freeze, R. A., & Witherspoon, P. A. (1967). Theoretical analysis of regional groundwater flow: 2. Effect of water-table configuration and subsurface permeability variation. *Water Resources Research*, *3*(2), 623–634. <https://doi.org/10.1029/WR003i002p00623>
- Gabrielli, C. P., McDonnell, J. J., & Jarvis, W. T. (2012). The role of bedrock groundwater in rainfall-runoff response at hillslope and catchment scales. *Journal of Hydrology*, *450–451*, 117–133. <https://doi.org/10.1016/j.jhydrol.2012.05.023>
- Gleeson, T., & Manning, A. H. (2008). Regional groundwater flow in mountainous terrain: Three-dimensional simulations of topographic and hydrogeologic controls. *Water Resources Research*, *44*, W10403. <https://doi.org/10.1029/2008WR006848>
- Graham, C. B., Barnard, H. R., Kavanagh, K. L., & McNamara, J. P. (2013). Catchment scale controls the temporal connection of transpiration and diel fluctuations in streamflow. *Hydrological Processes*, *27*(18), 2541–2556. <https://doi.org/10.1002/hyp.9334>
- Hahm, W. J., Rempe, D. M., Dralle, D. N., Dawson, T. E., Lovill, S. M., Bryk, A. B., et al. (2019). Lithologically controlled subsurface critical zone thickness and water storage capacity determine regional plant community composition. *Water Resources Research*, *55*, 3028–3055. <https://doi.org/10.1029/2018WR023760>
- Harr, R. D. (1977). Water flux in soil and subsoil on a steep forested slope. *Journal of Hydrology*, *33*(1–2), 37–58. [https://doi.org/10.1016/0022-1694\(77\)90097-X](https://doi.org/10.1016/0022-1694(77)90097-X)

- Harr, R. D., Robert D., Ranken, D. W., Biome, U. S. I. B. P. C. F., & Washington, U. of. (1972). Movement of water through forested soils in steep topography. Retrieved from <http://ir.library.oregonstate.edu/xmlui/handle/1957/7777>
- Harrington, C. A., Holub, S. M., Bauer, C., & Steel, E. A. (2017). The distribution of tree roots in Douglas-fir forests in the Pacific Northwest in relation to depth, space, coarse organic matter and mineral fragments. *Northwest Science*, 91(4), 326–343. <https://doi.org/10.3955/046.091.0403>
- Hasenmueller, E. A., Gu, X., Weitzman, J. N., Adams, T. S., Stinchcomb, G. E., Eissenstat, D. M., et al. (2017). Weathering of rock to regolith: The activity of deep roots in bedrock fractures. *Geoderma*, 300, 11–31. <https://doi.org/10.1016/J.GEODERMA.2017.03.020>
- Hasselquist, N. J., Allen, M. F., & Santiago, L. S. (2010). Water relations of evergreen and drought-deciduous trees along a seasonally dry tropical forest chronosequence. *Oecologia*, 164(4), 881–890. <https://doi.org/10.1007/s00442-010-1725-y>
- Hermann, R., & Lavender, D. (1990). *Pseudotsuga menziesii* (Mirb.) Franco. (Silvics of). Department of Agriculture Forest Service, Washington, D.C.
- Kramer, P. J., & Boyer, J. S. (1995). *Water Relation of Plants and Soils*. London: Academic Press.
- Klos, P. Z., Goulden, M. L., Riebe, C. S., Tague, C. L., O'Geen, A. T., Flinchum, B. A., et al. (2018). Subsurface plant-accessible water in mountain ecosystems with a Mediterranean climate. *Wiley Interdisciplinary Reviews Water*, 5(3), e1277. <https://doi.org/10.1002/wat2.1277>
- Loheide, S. P. II (2008). A method for estimating subdaily evapotranspiration of shallow groundwater using diurnal water table fluctuations. *Ecohydrology*, 1(1), 59–66. <https://doi.org/10.1002/eco.7>
- Lundquist, J. D., & Cayan, D. R. (2002). Seasonal and Spatial Patterns in Diurnal Cycles in Streamflow in the Western United States. *Journal of Hydrometeorology*, 3(5), 591–603. [https://doi.org/10.1175/1525-7541\(2002\)0032.0.co;2](https://doi.org/10.1175/1525-7541(2002)0032.0.co;2)
- Lundquist, J. D., Cayan, D. R., Lundquist, J. D., & Cayan, D. R. (2002). Seasonal and spatial patterns in diurnal cycles in streamflow in the western United States. *Journal of Hydrometeorology*, 3(5), 591–603. [https://doi.org/10.1175/1525-7541\(2002\)003<0591:SASPID>2.0.CO;2](https://doi.org/10.1175/1525-7541(2002)003<0591:SASPID>2.0.CO;2)
- Marshall, D. C. (1958). Measurement of sap flow in conifers by heat transport. *Plant Physiology*, 33(6), 385–96. Retrieved from <http://www.ncbi.nlm.nih.gov/pubmed/16655154>
- McDonnell, J. J., McGuire, K., Aggarwal, P., Beven, K. J., Biondi, D., Destouni, G., et al. (2010). How old is streamwater? Open questions in catchment transit time conceptualization, modelling and analysis. *Hydrological Processes*, 24(12), 1745–1754. <https://doi.org/10.1002/hyp.7796>
- McDowell, N. G., Phillips, N., Lunch, C., Bond, B. J., & Ryan, M. G. (2002). An investigation of hydraulic limitation and compensation in large, old Douglas-fir trees. *Tree Physiology*, 22(11), 763–774. <https://doi.org/10.1093/treephys/22.11.763>
- McGuire, K. J., Weiler, M., & McDonnell, J. J. (2007). Integrating tracer experiments with modeling to assess runoff processes and water transit times. *Advances in Water Resources*, 30(4), 824–837. <https://doi.org/10.1016/j.advwatres.2006.07.004>
- Miles, P. D., & Smith, W. B. (2009). Specific gravity and other properties of wood and bark for 156 tree species found in North America. *Res. Note NRS-38. US Department of Agriculture Forest Service, Northern Research Station* (Vol. 10). Newtown Square, PA, USA.
- Moore, G. W., Jones, J. A., & Bond, B. J. (2011). How soil moisture mediates the influence of transpiration on streamflow at hourly to interannual scales in a forested catchment. *Hydrological Processes*, 25(24), 3701–3710. <https://doi.org/10.1002/hyp.8095>
- Moore, M. F., Vasconcelos, J. G., Zech, W. C., & Soares, E. P. (2016). A procedure for resolving thermal artifacts in pressure transducers. *Flow Measurement and Instrumentation*, 52, 219–226. <https://doi.org/10.1016/j.flowmeasinst.2016.10.010>
- Poot, P., Hopper, S. D., & van Diggelen, J. M. H. (2012). Exploring rock fissures: Does a specialized root morphology explain endemism on granite outcrops? *Annals of Botany*, 110(2), 291–300. <https://doi.org/10.1093/aob/mcr322>
- PRISM Climate Group (2017). Oregon State University [internet]. Descriptions of PRISM spatial climate datasets for the conterminous United States. [Available at [http://www.prism.oregonstate.edu/documents/PRISM\\_datasets.pdf](http://www.prism.oregonstate.edu/documents/PRISM_datasets.pdf), (Cited 25 October 2017).]
- Ranken, D. W., & Wesley, D. (1974). Hydrologic properties of soil and subsoil on a steep, forested slope. Retrieved from <http://ir.library.oregonstate.edu/xmlui/handle/1957/9767>
- Rempe, D. M., & Dietrich, W. E. (2014). A bottom-up control on fresh-bedrock topography under landscapes. *Proceedings of the National Academy of Sciences of the United States of America*, 111(18), 6576–6581. <https://doi.org/10.1073/pnas.1404763111>
- Rempe, D. M., & Dietrich, W. E. (2018). Direct observations of rock moisture, a hidden component of the hydrologic cycle. *Proceedings of the National Academy of Sciences*, 115(11), 2664–2669.
- Richards, J. H., & Caldwell, M. M. (1987). Hydraulic lift: Substantial nocturnal water transport between soil layers by *Artemisia tridentata* roots. *Oecologia*, 73(4), 486–489. <https://doi.org/10.1007/BF00379405>
- Shanley, J. B., Hjerdt, K. N., McDonnell, J. J., & Kendall, C. (2003). Shallow water table fluctuations in relation to soil penetration resistance. *Ground Water*, 41(7), 964–972. <https://doi.org/10.1111/j.1745-6584.2003.tb02438.x>
- Sollins, P., Cromack, K., Mc Corison, F. M., Waring, R. H., & Harr, R. D. (1981). Changes in nitrogen cycling at an old-growth Douglas-fir site after Disturbance1. *Journal of Environmental Quality*, 10(1), 37. <https://doi.org/10.2134/jeq1981.00472425001000010007x>
- Starr, J. L., & Paltineanu, I. C. (2002). Methods for measurement of soil water content: Capacitance devices. *Methods of Soil Analysis: Part, 4*.
- Steppe, K., De Pauw, D. J. W., Doody, T. M., & Teskey, R. O. (2010). A comparison of sap flux density using thermal dissipation, heat pulse velocity and heat field deformation methods. *Agricultural and Forest Meteorology*, 150(7–8), 1046–1056. <https://doi.org/10.1016/j.agrformet.2010.04.004>
- Swanson, F. J., Frederick, J., & James, M. E. (1975). Geology and geomorphology of the H.J. Andrews Experimental Forest, Western Cascades, Oregon. Pacific Northwest Forest and Range Experiment Station, Forest service, U.S. Dept. of Agriculture. Retrieved from <http://agris.fao.org/agris-search/search.do?recordID=US201300715326>
- Swanson, R. H., & Whitfeild, D. W. A. (1981). A numerical analysis of heat pulse velocity theory and practice. *Journal of Experimental Botany*, 32(1), 221–239. <https://doi.org/10.1093/jxb/32.1.221>
- Széles, B., Broer, M., Parajka, J., Hogan, P., Eder, A., Strauss, P., & Blöschl, G. (2018). Separation of scales in transpiration effects on low flows: A spatial analysis in the hydrological open air laboratory. *Water Resources Research*, 54, 6168–6188. <https://doi.org/10.1029/2017WR022037>
- Szilágyi, J., Gribovszki, Z., Kalicz, P., & Kucsara, M. (2008). On diurnal riparian zone groundwater-level and streamflow fluctuations. *Journal of Hydrology*, 349(1–2), 1–5. <https://doi.org/10.1016/j.jhydrol.2007.09.014>
- Tóth, J. (1963). A theoretical analysis of groundwater flow in small drainage basins. *Journal of Geophysical Research*, 68(16), 4795–4812. <https://doi.org/10.1029/jz068i016p04795>
- Turk, L. J. (1975). Diurnal fluctuations of water tables induced by atmospheric pressure changes. *Journal of Hydrology*, 26(1–2), 1–16.

- Van Verseveld, W. J., Barnard, H. R., Graham, C. B., McDonnell, J. J., Renée Brooks, J., & Weiler, M. (2017). A sprinkling experiment to quantify celerity-velocity differences at the hillslope scale. *Hydrology and Earth System Sciences*, *21*(11), 5891–5910. <https://doi.org/10.5194/hess-21-5891-2017>
- van Verseveld, W. J., McDonnell, J. J., & Lajtha, K. (2009). The role of hillslope hydrology in controlling nutrient loss. *Journal of Hydrology*, *367*(3–4), 177–187. <https://doi.org/10.1016/j.jhydrol.2008.11.002>
- Voytek, E. B., Barnard, H. R., Jougnot, D., & Singha, K. (2019). Transpiration- and precipitation-induced subsurface water flow observed using the self-potential method. *Hydrological Processes*. <https://doi.org/10.1002/hyp.13453>
- Warren, J. M., Meinzer, F. C., Brooks, J. R., & Domec, J. C. (2005). Vertical stratification of soil water storage and release dynamics in Pacific Northwest coniferous forests. *Agricultural and Forest Meteorology*, *130*(1–2), 39–58. <https://doi.org/10.1016/j.agrformet.2005.01.004>
- Winter, T. C. (2001). Ground water and surface water: the linkage tightens, but challenges remain. *Hydrological Processes*, *15*(18), 3605–3606. <https://doi.org/10.1002/hyp.504>
- Witty, J. H., Graham, R. C., Hubbert, K. R., Doolittle, J. A., & Wald, J. A. (2003). Contributions of water supply from the weathered bedrock zone to forest soil quality. *Geoderma*, *114*(3–4), 389–400. [https://doi.org/10.1016/S0016-7061\(03\)00051-X](https://doi.org/10.1016/S0016-7061(03)00051-X)
- Wondzell, S. M., Gooseff, M. N., & McGlynn, B. L. (2009). An analysis of alternative conceptual models relating hyporheic exchange flow to diel fluctuations in discharge during baseflow recession. *Hydrological Processes*, *24*(6), 686–694. <https://doi.org/10.1002/hyp.7507>
- White, W. N. (1932). A method of estimating ground-water supplies based on discharge by plants and evaporation from soil. *Results of investigation in Escalante Valley, Utah. US Geological Survey Water Supply Paper:1-105*.
- Yano, Y., Lajtha, K., Sollins, P., & Caldwell, B. A. (2005). Chemistry and dynamics of dissolved organic matter in a temperate coniferous forest on Andic soils: Effects of litter quality. *Ecosystems*, *8*(3), 286–300. <https://doi.org/10.1007/s10021-005-0022-9>
- Yashi, D. K., Suzuki, K., & Nomura, M. (1990). Diurnal fluctuation in stream flow and in specific electric conductance during drought periods. *Journal of Hydrology*, *115*(1–4), 105–114. [https://doi.org/10.1016/0022-1694\(90\)90200-H](https://doi.org/10.1016/0022-1694(90)90200-H)